The Neutrino Roof: Single-Scatter Ceilings in Dark Matter Direct Searches

Nirmal Raj

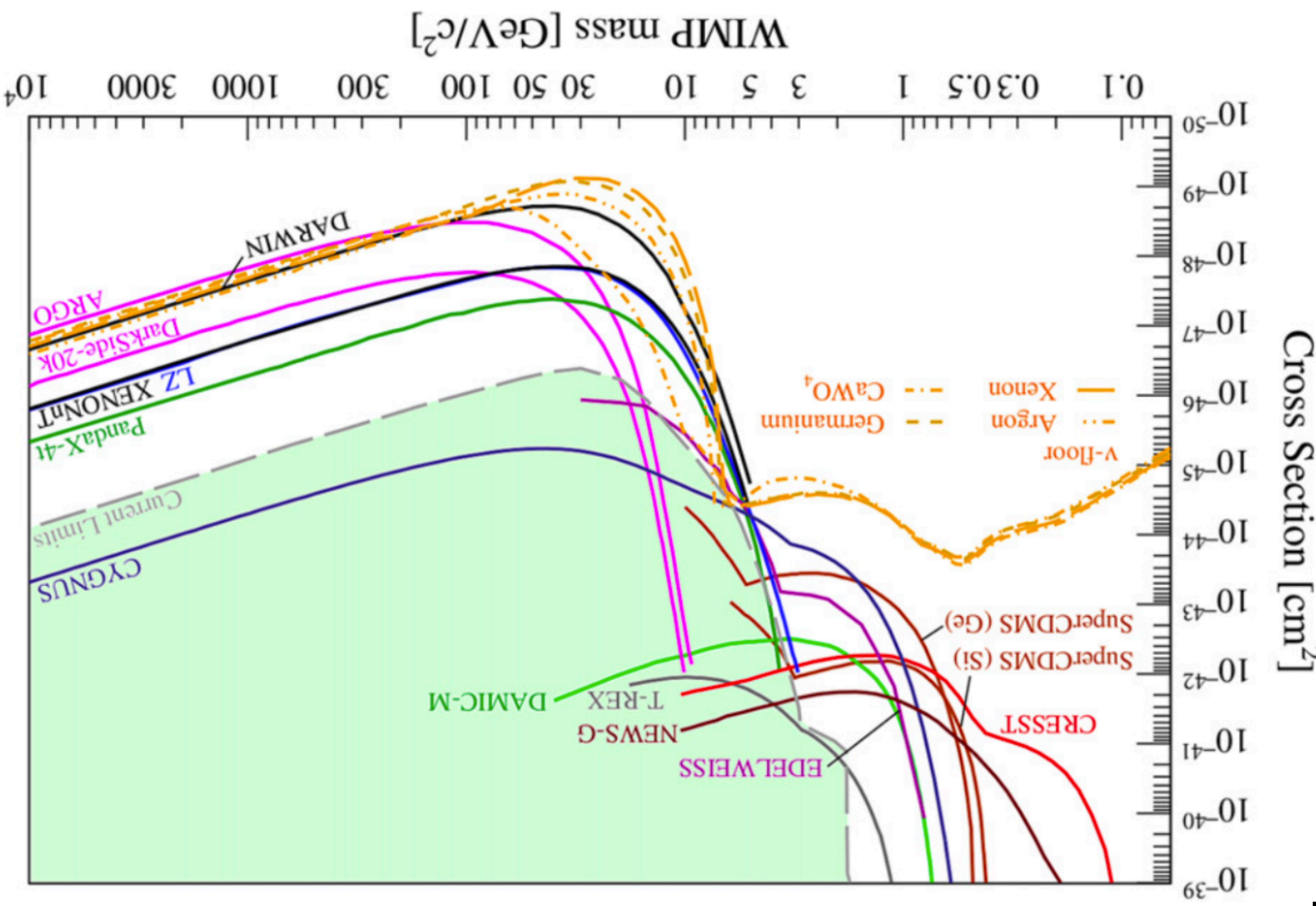

<u>collaborators</u>

Joe Bramante, Ben Broerman,
Shivam Garg, Jason Kumar,
Michela Lai, Rafael Lang,
Biprajit Mondal,
Maxim Pospelov, Shawn Westerdale

Indian Institute of Science
Indian Institute of Technology Hyderabad

PPC 2024, 17 Oct 2024

Punchline for experts

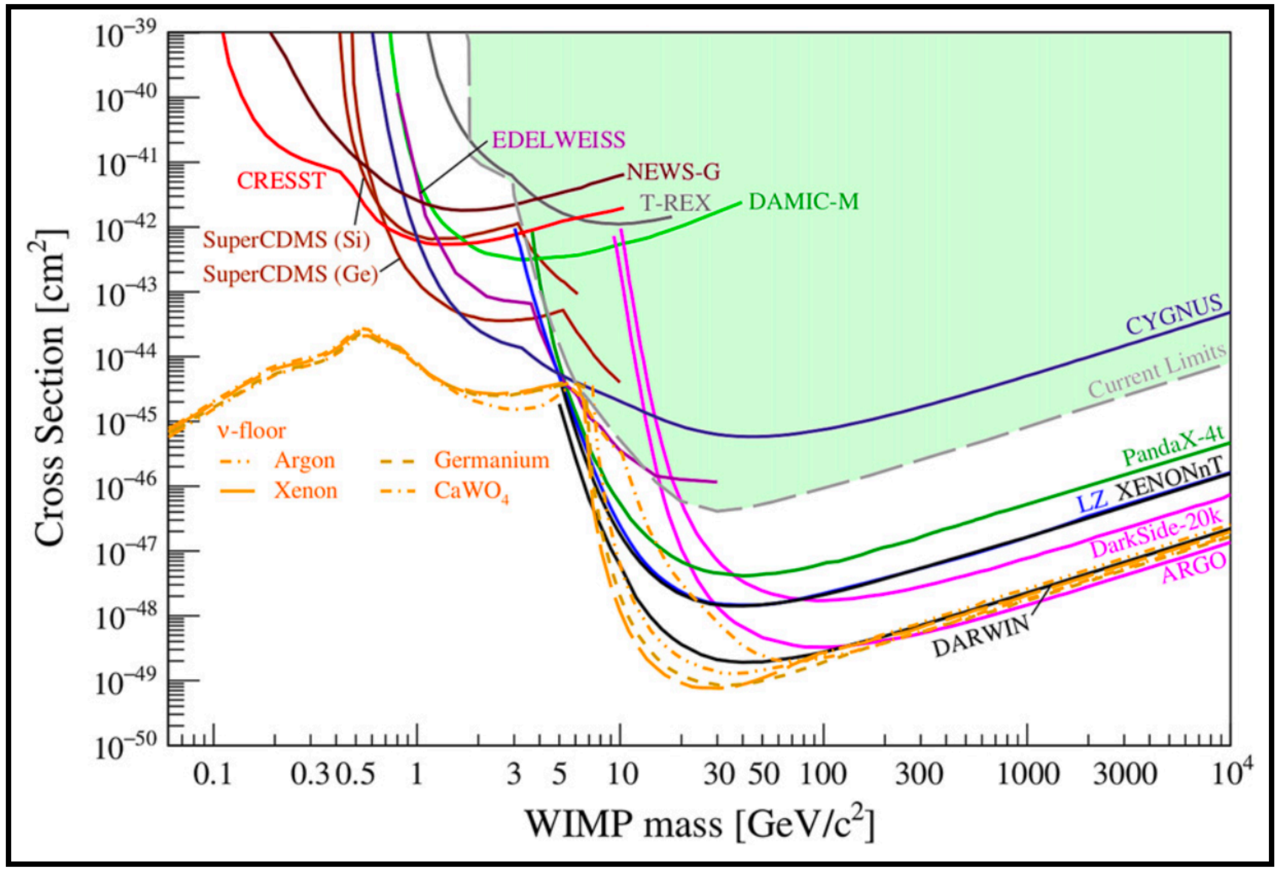

APPEC report, 2104.07634

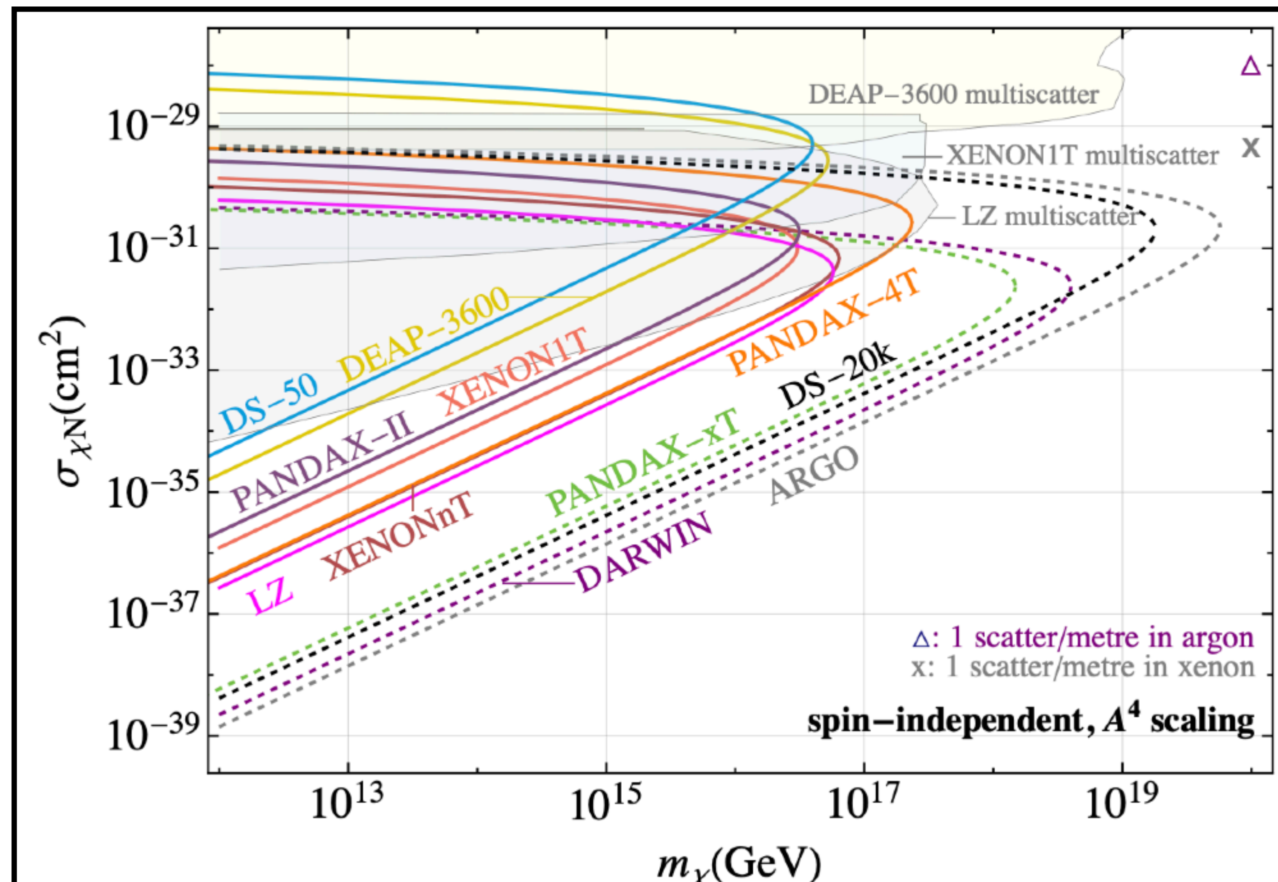

Raj & Mondal, 2406.17015

Dark reality

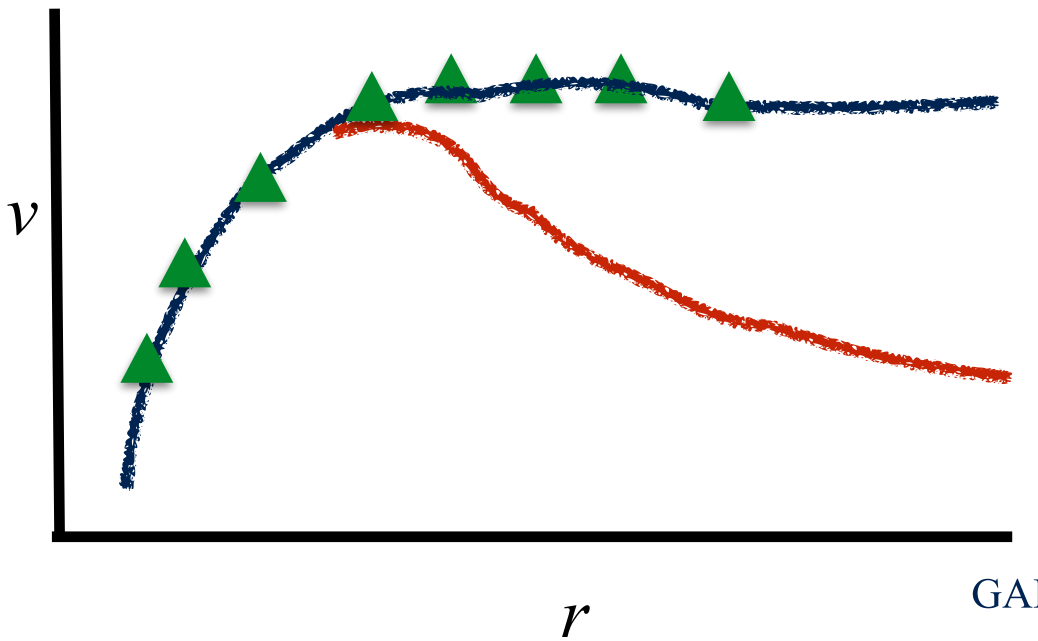

GALACTIC ROTATION

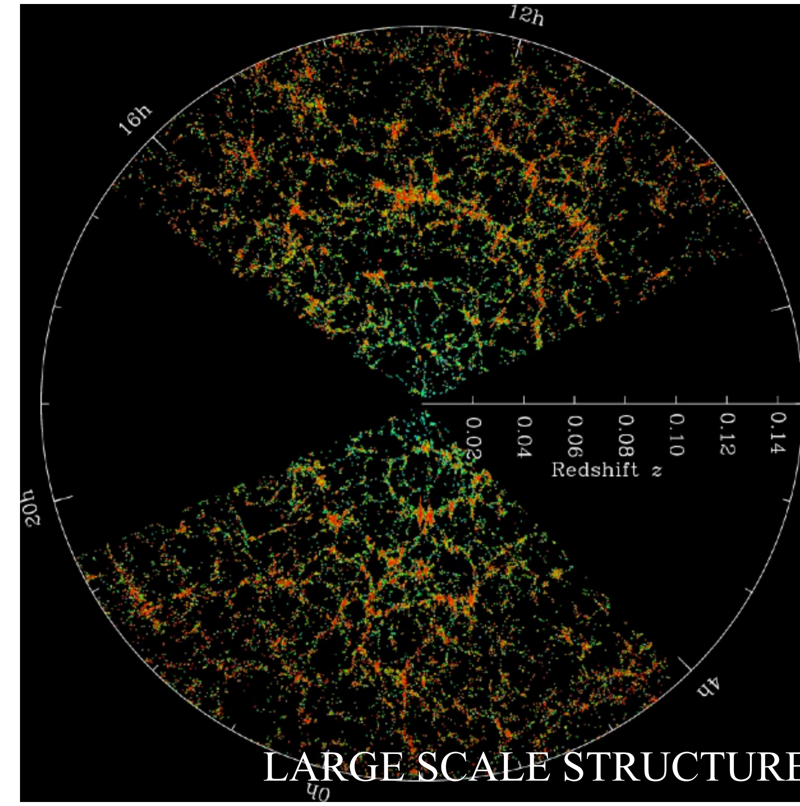

LARGE SCALE STRUCTURE

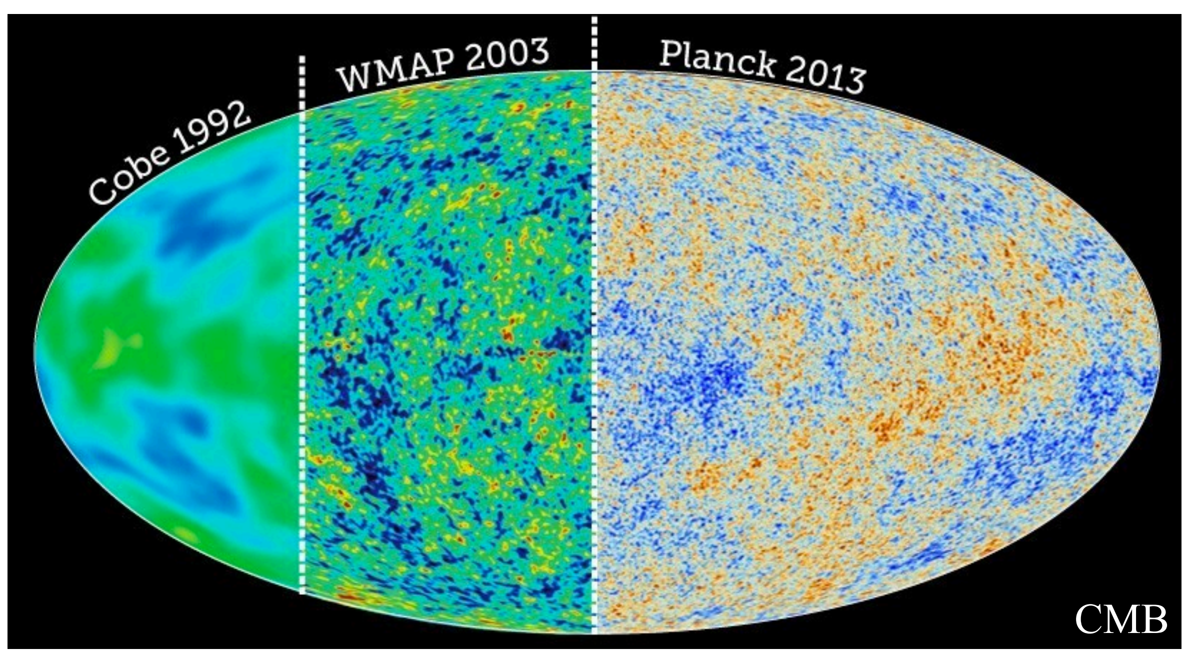

CMB

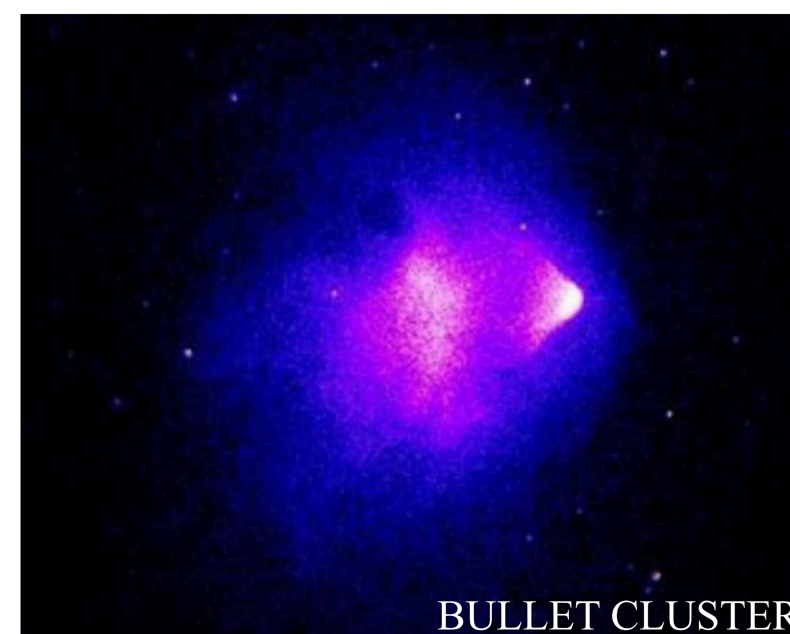

BULLET CLUSTER

Direct detection: the beginning

PHYSICAL REVIEW D VOLUME 31, NUMBER 12 15 JUNE 1985

Detectability of certain dark-matter candidates

Mark W. Goodman and Edward Witten
Joseph Henry Laboratories, Princeton University, Princeton, New Jersey 08544

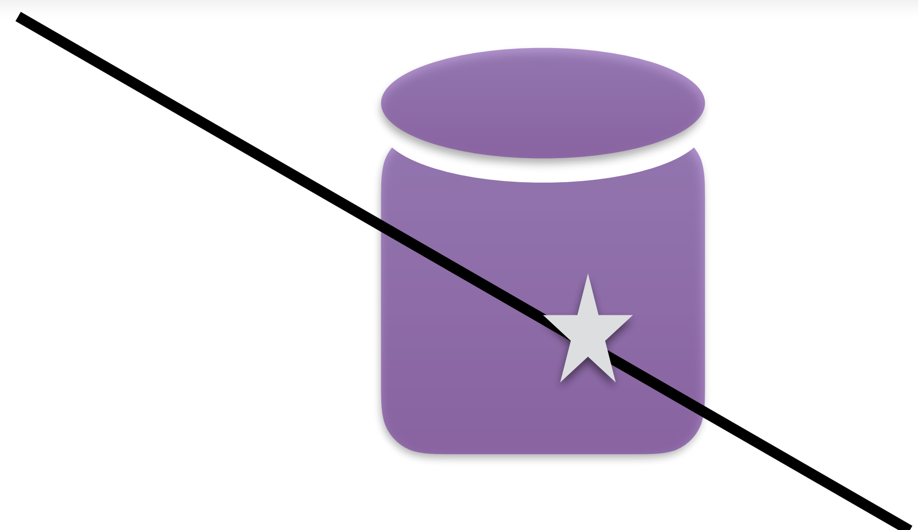

Encounter rate (spin-independent) =

$$6.8 \text{ events } \times \left(\frac{\sigma_{\chi N}}{10^{-39}\ \mathrm{cm}^2}\right)\left(\frac{A}{27}\right)^4\left(\frac{1000\ \mathrm{GeV}}{m_{\mathrm{DM}}}\right)\left(\frac{27}{A}\right)\left(\frac{\rho_{\mathrm{DM}}}{0.3\ \mathrm{GeV/cm}^3}\right)\left(\frac{v_{\mathrm{DM}}}{220\ \mathrm{km/s}}\right) /\mathrm{kg/day}$$

Preview: modern searches

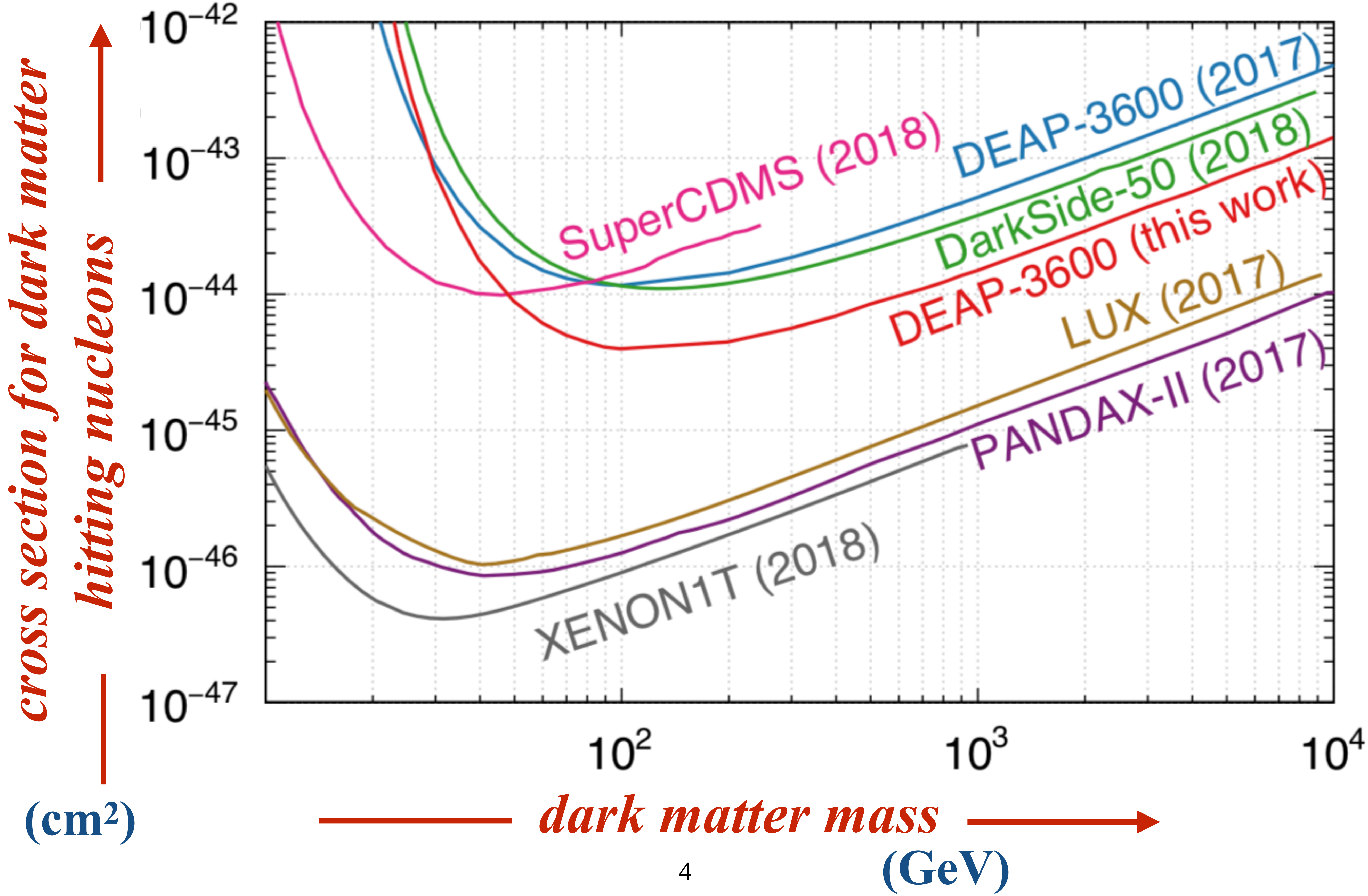

Direct detection status

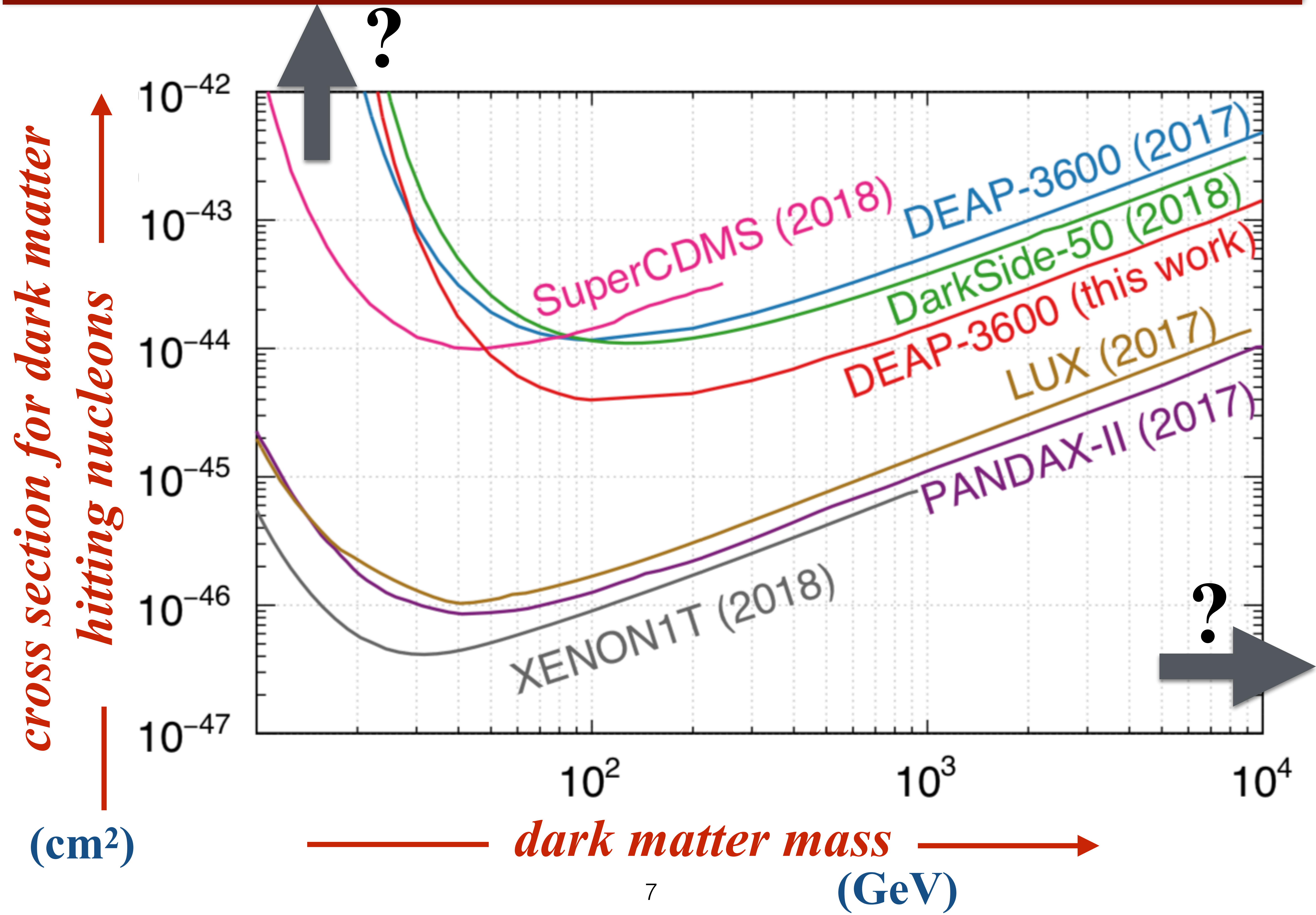

Bird's-eye view

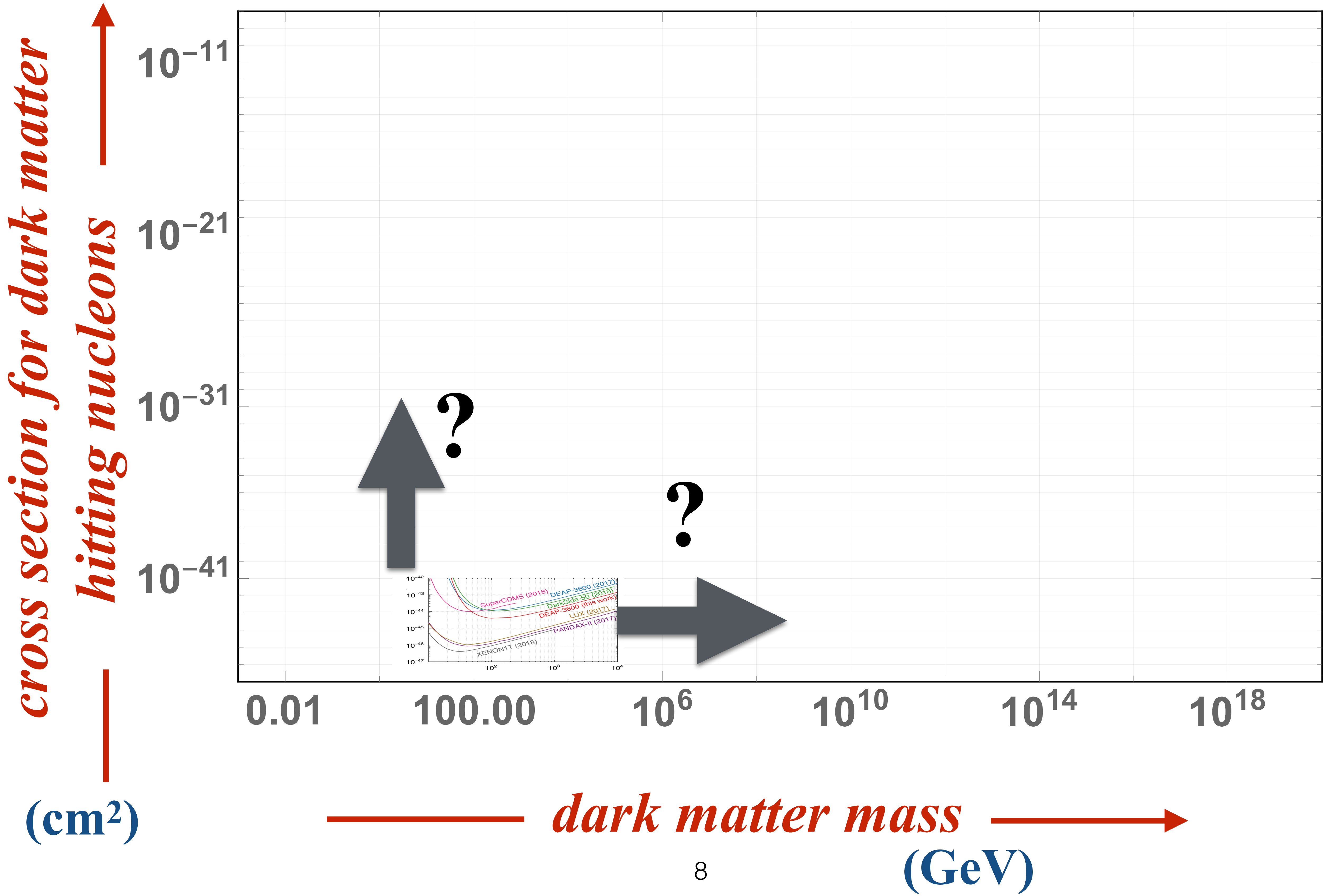

An educated guess

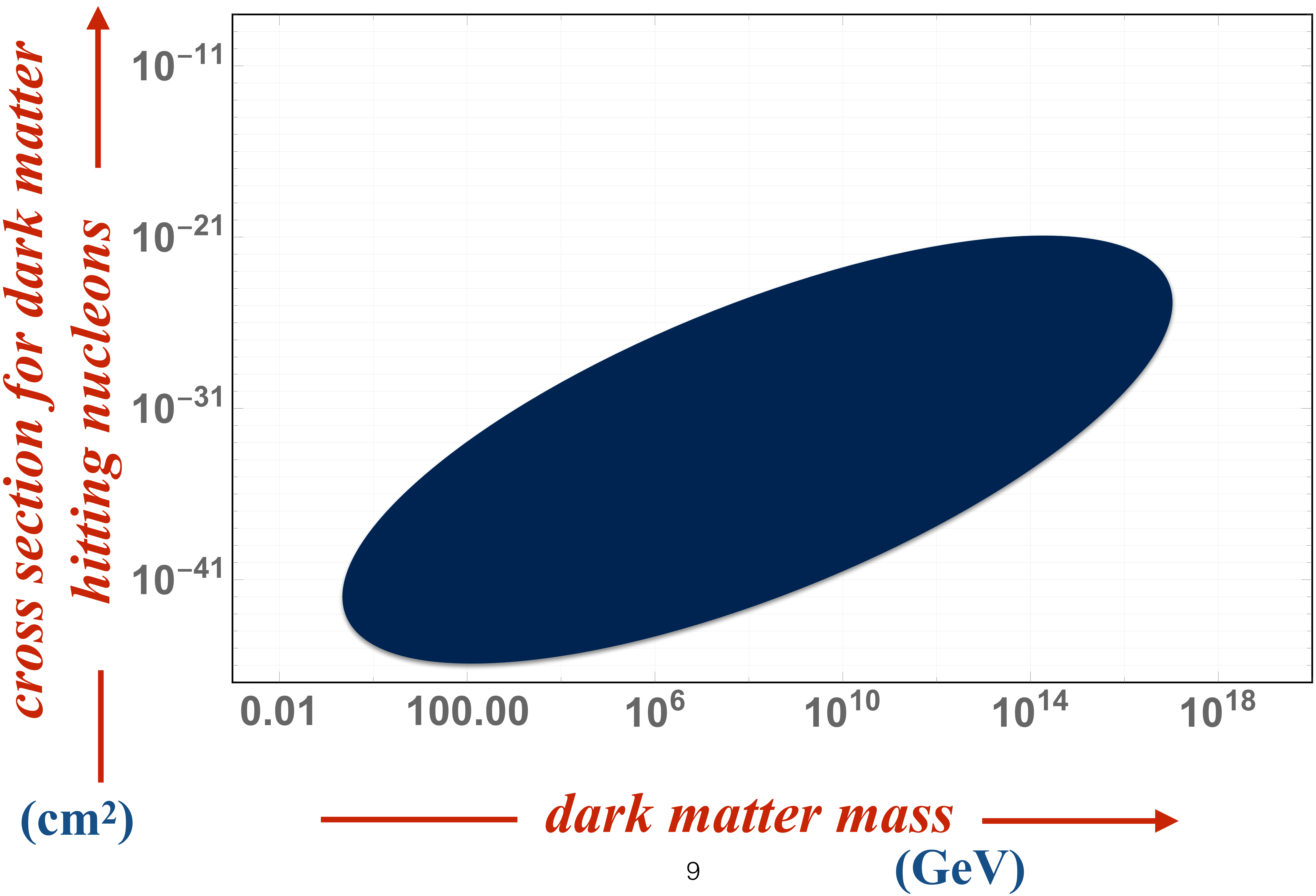

The four frontiers

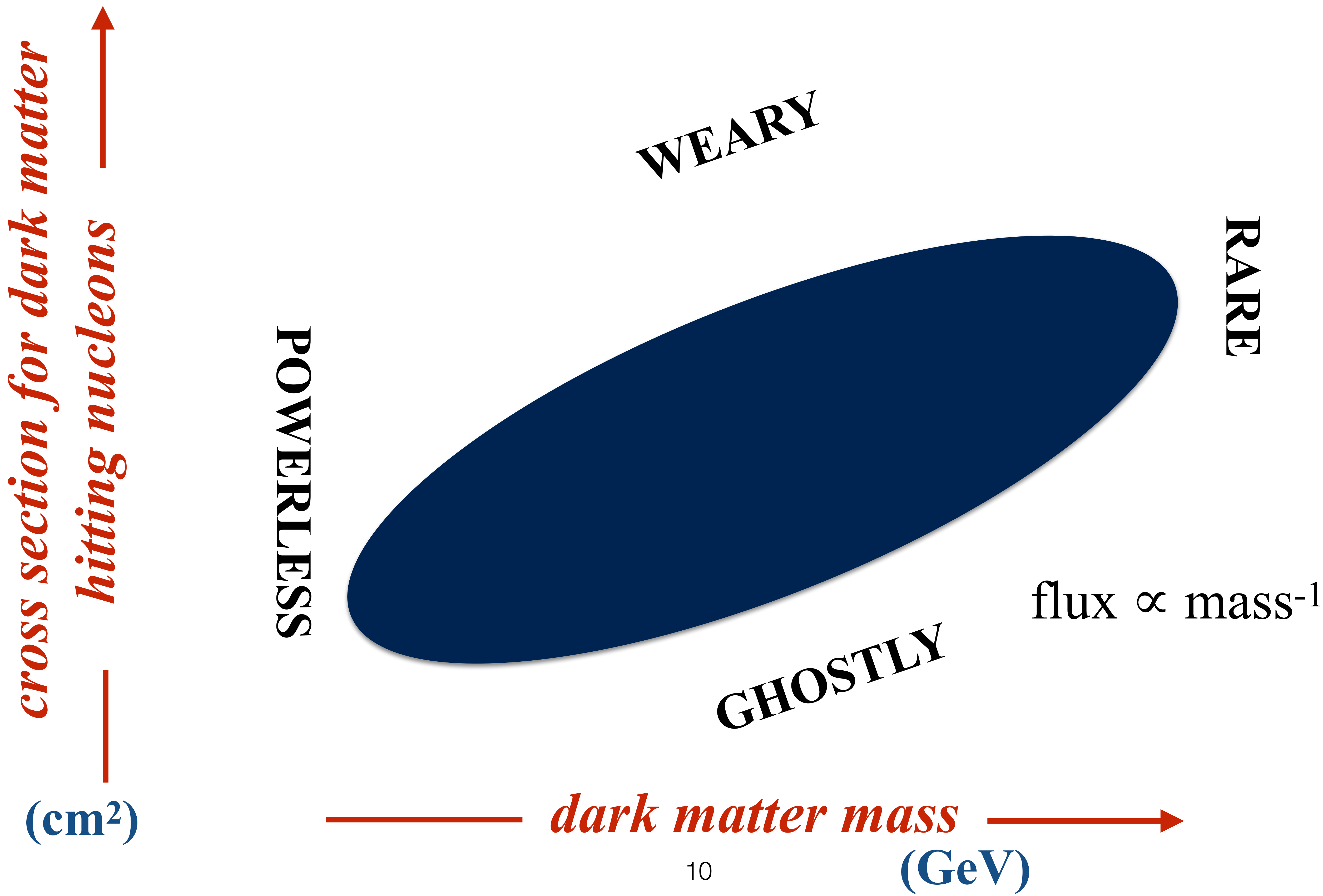

All the Earth-based constraints

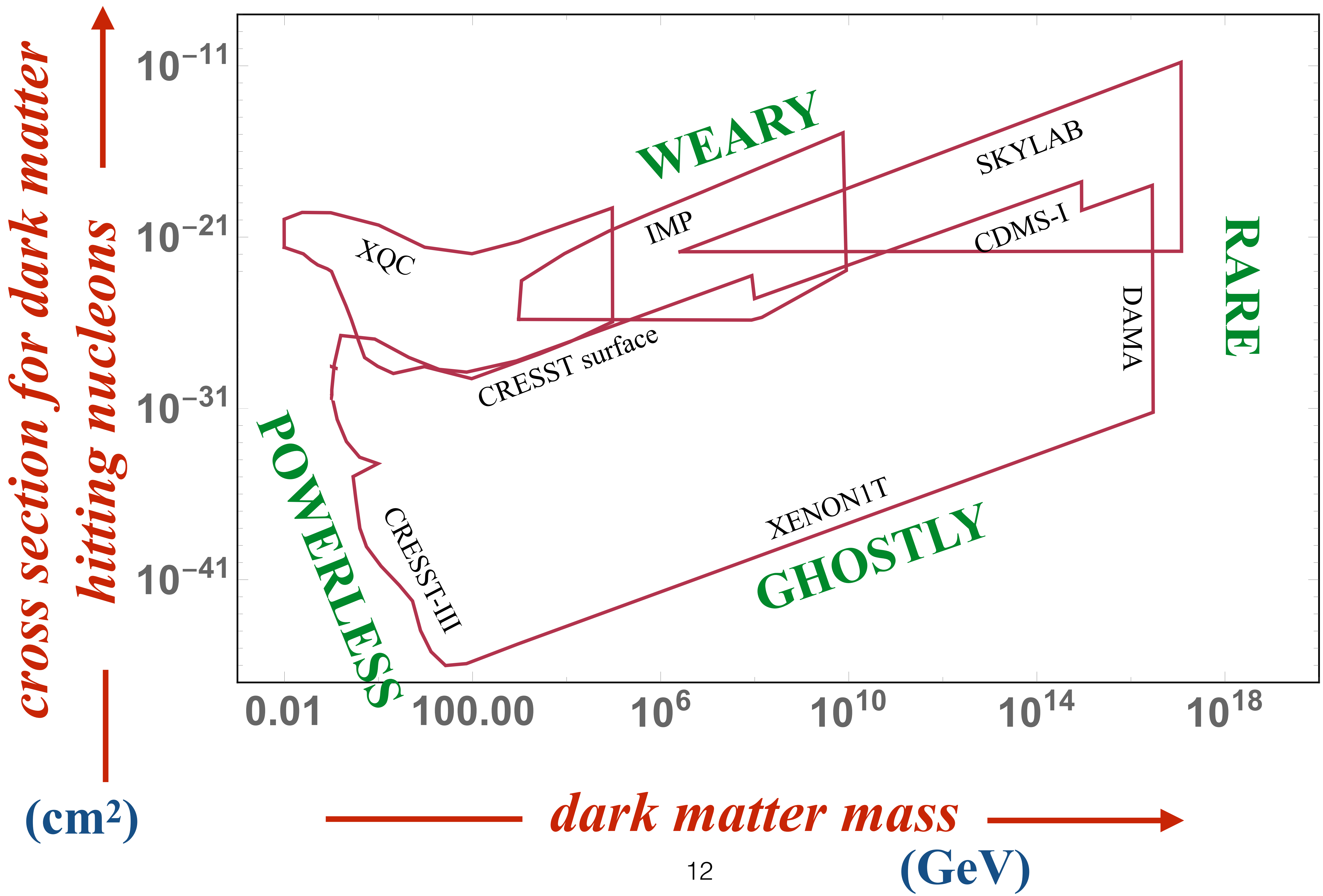

All the Earth-based constraints

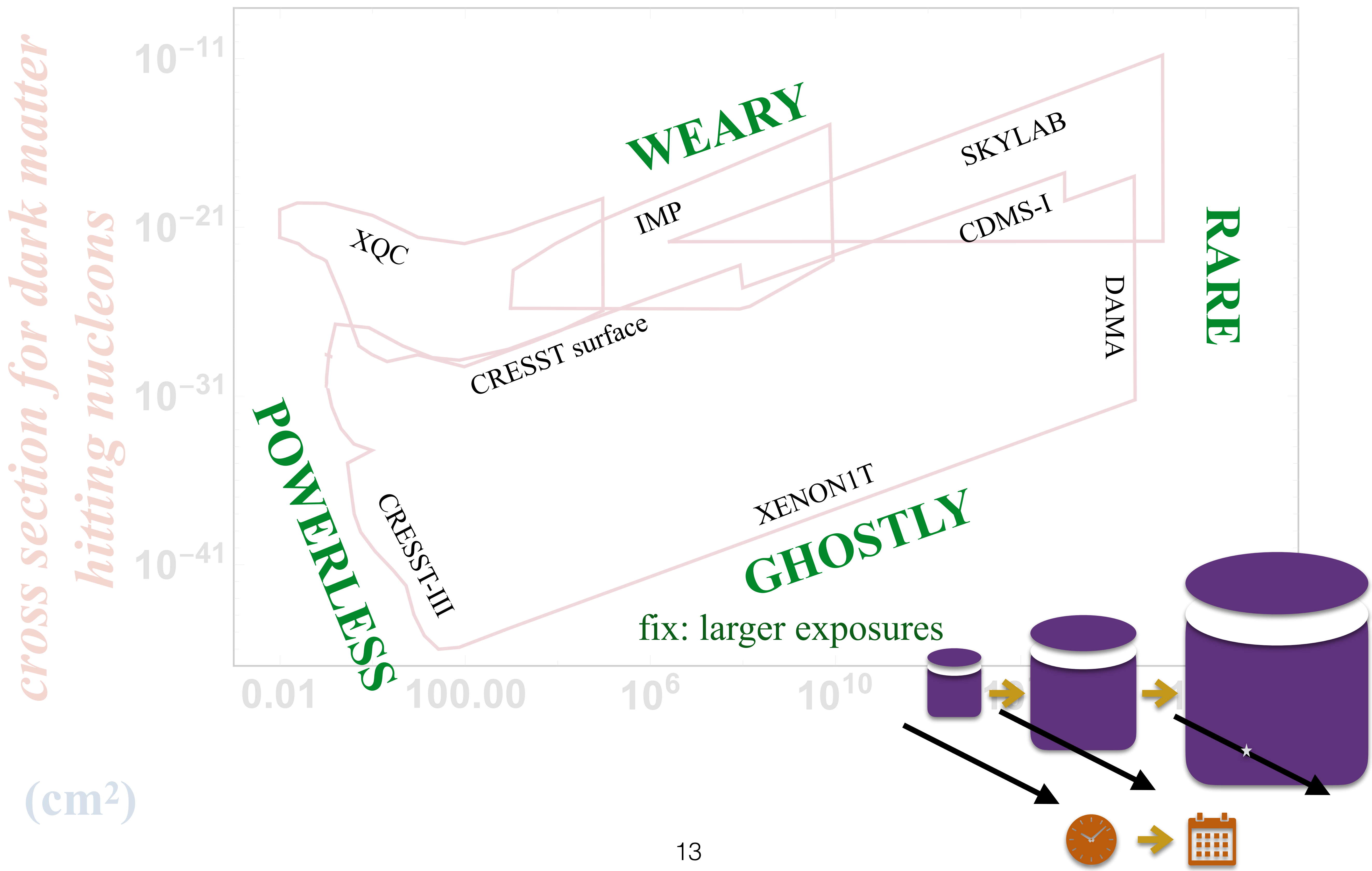

All the Earth-based constraints

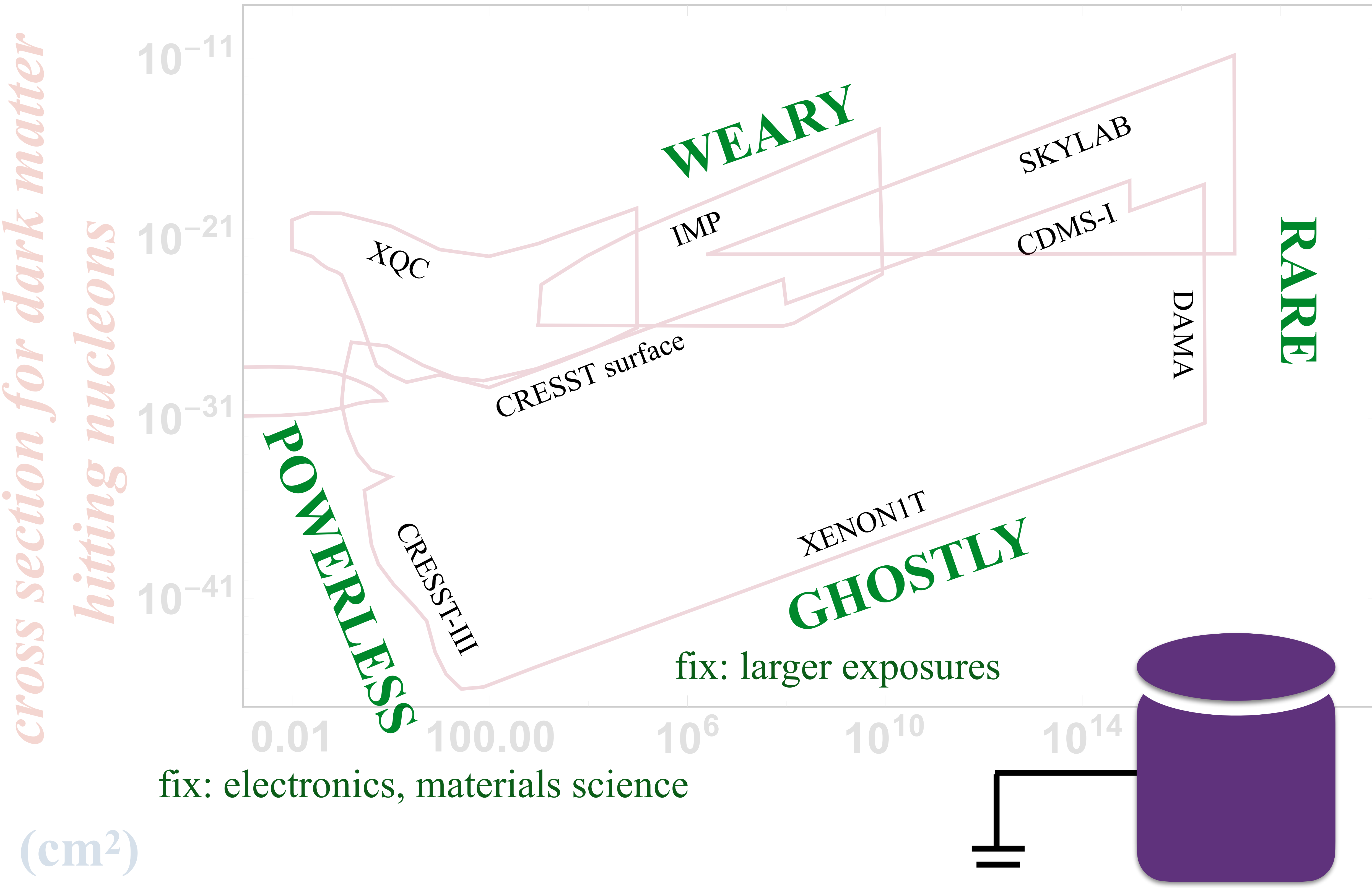

All the Earth-based constraints

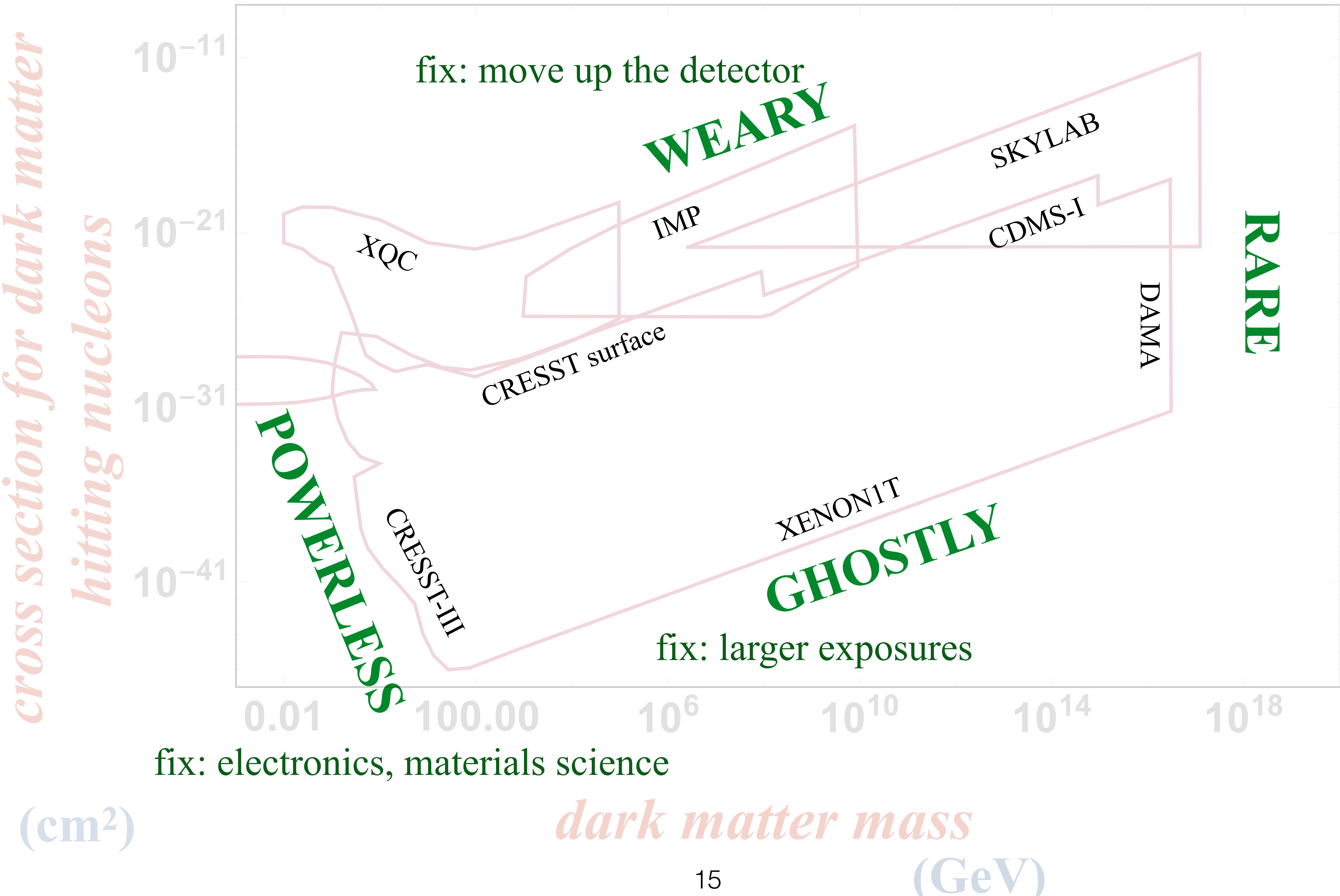

All the Earth-based constraints

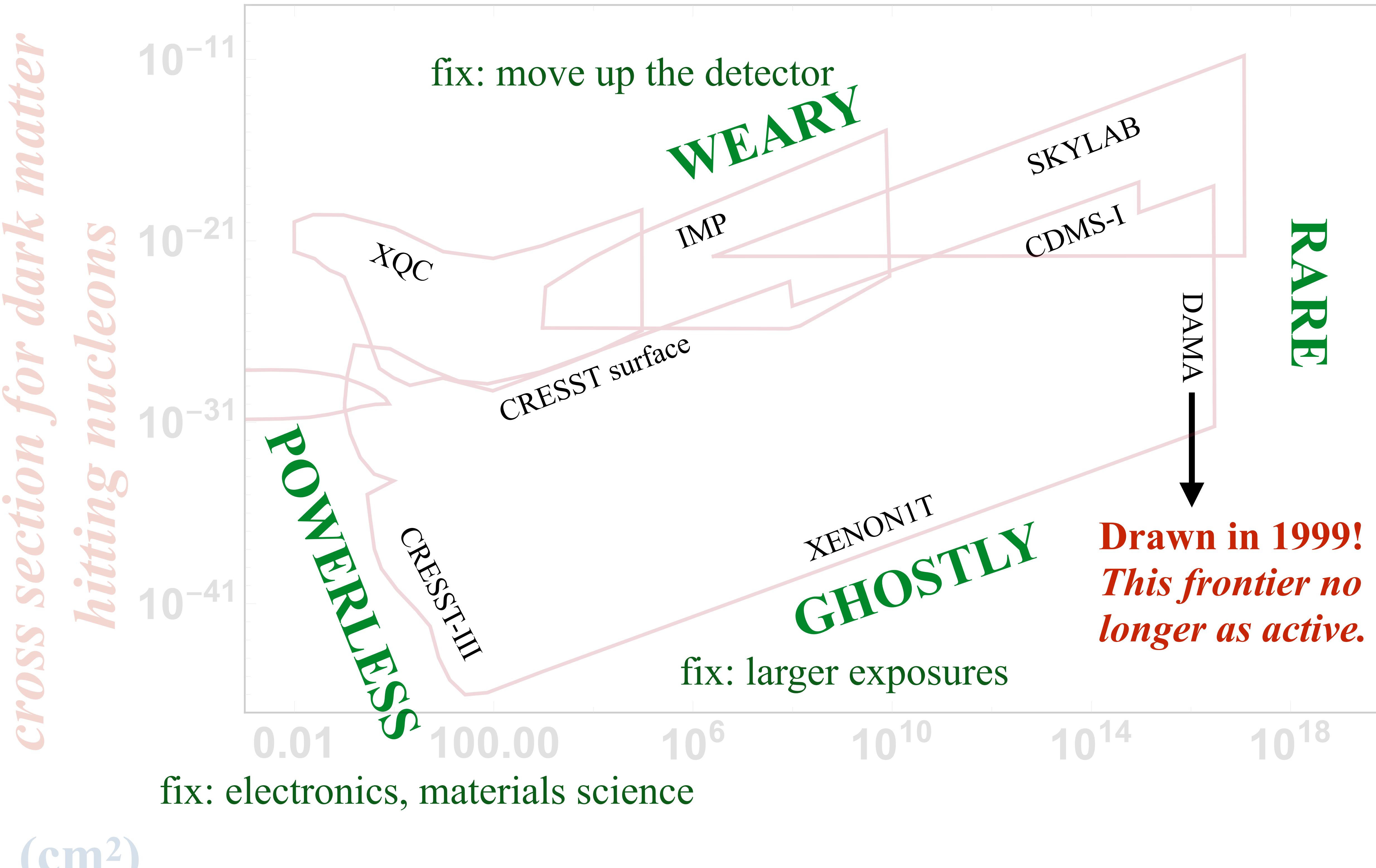

Drawn in 1999!
This frontier no longer as active.

Profusion

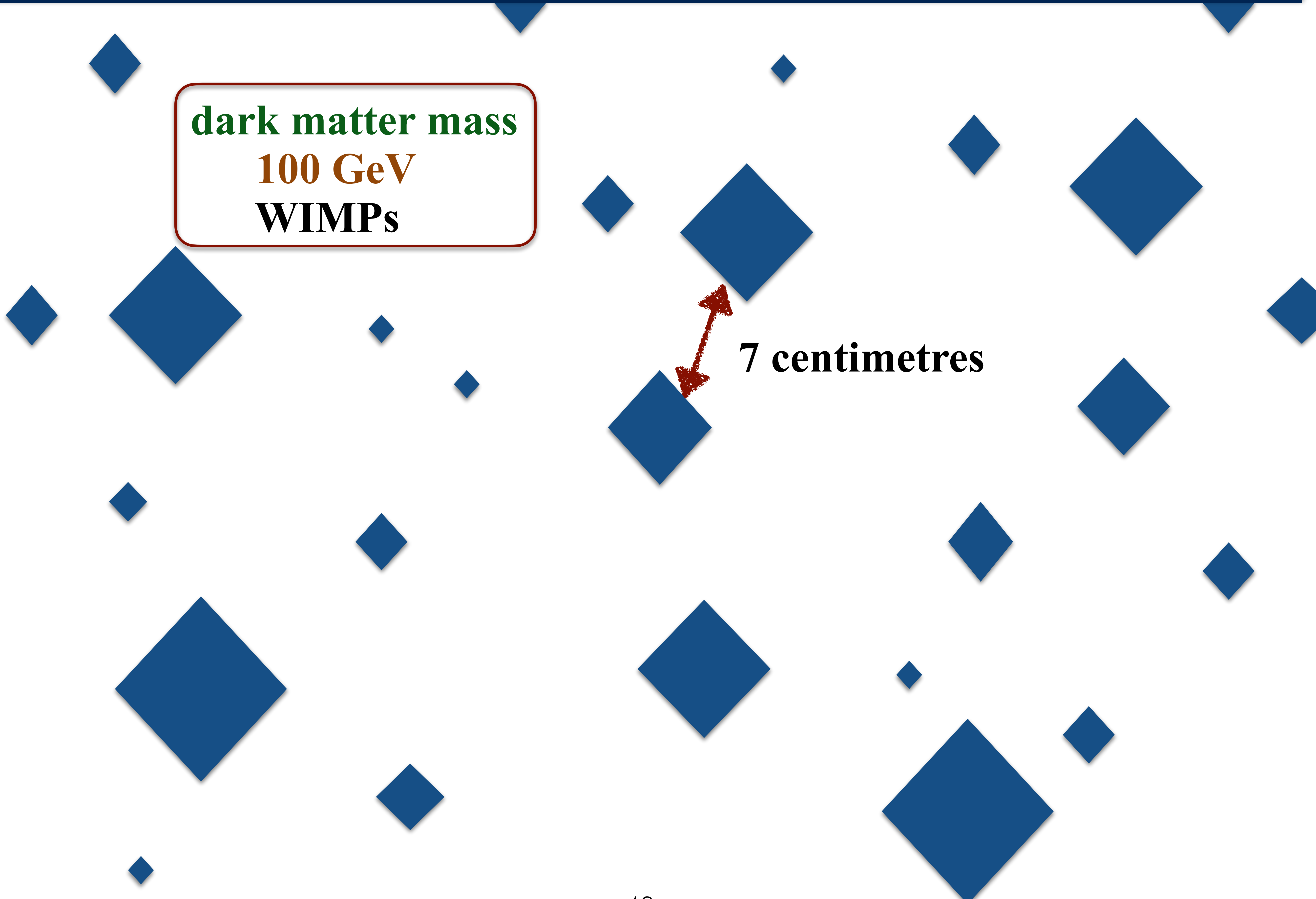

Rarity

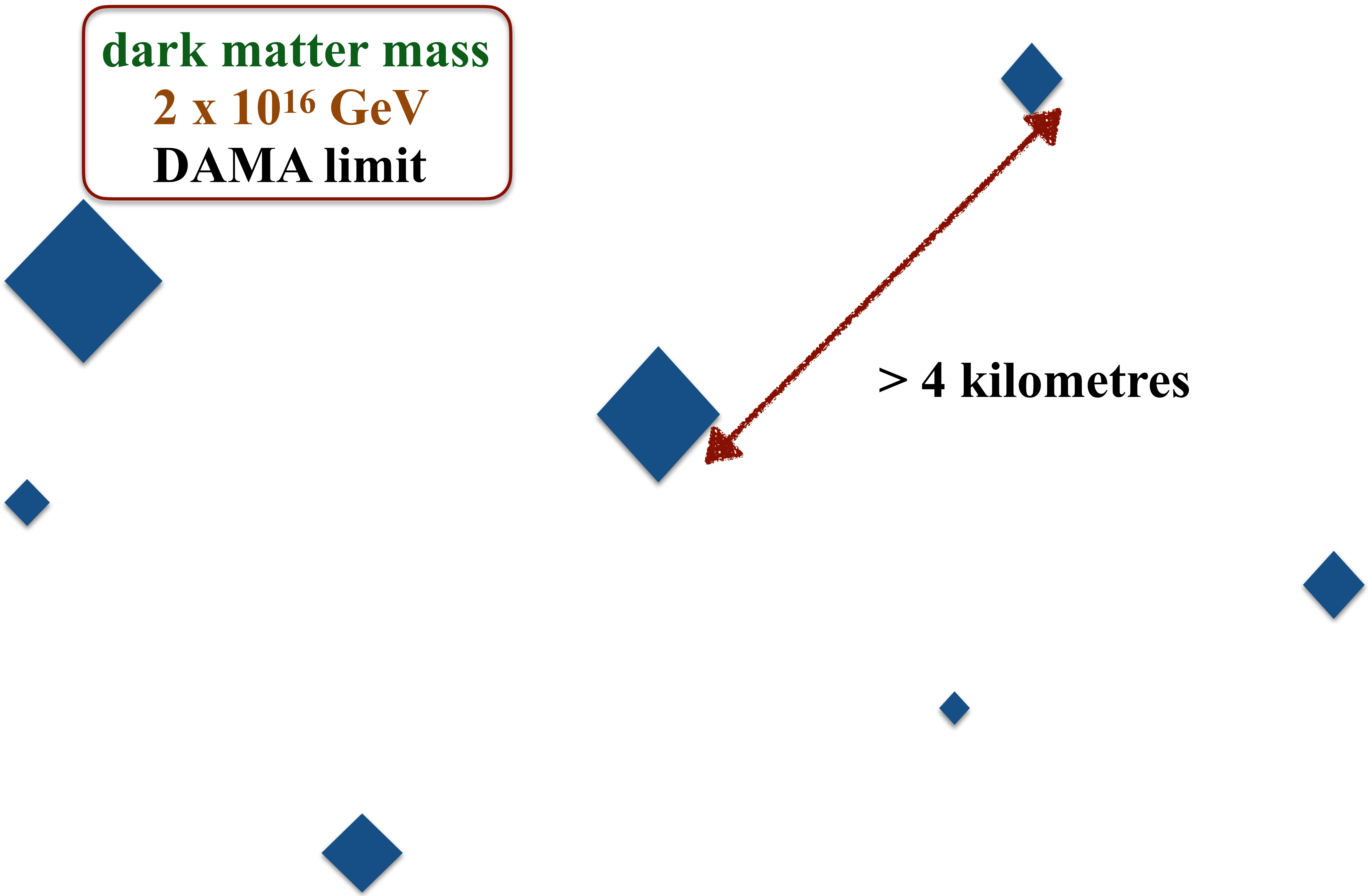

Hunting even rarer dark matter

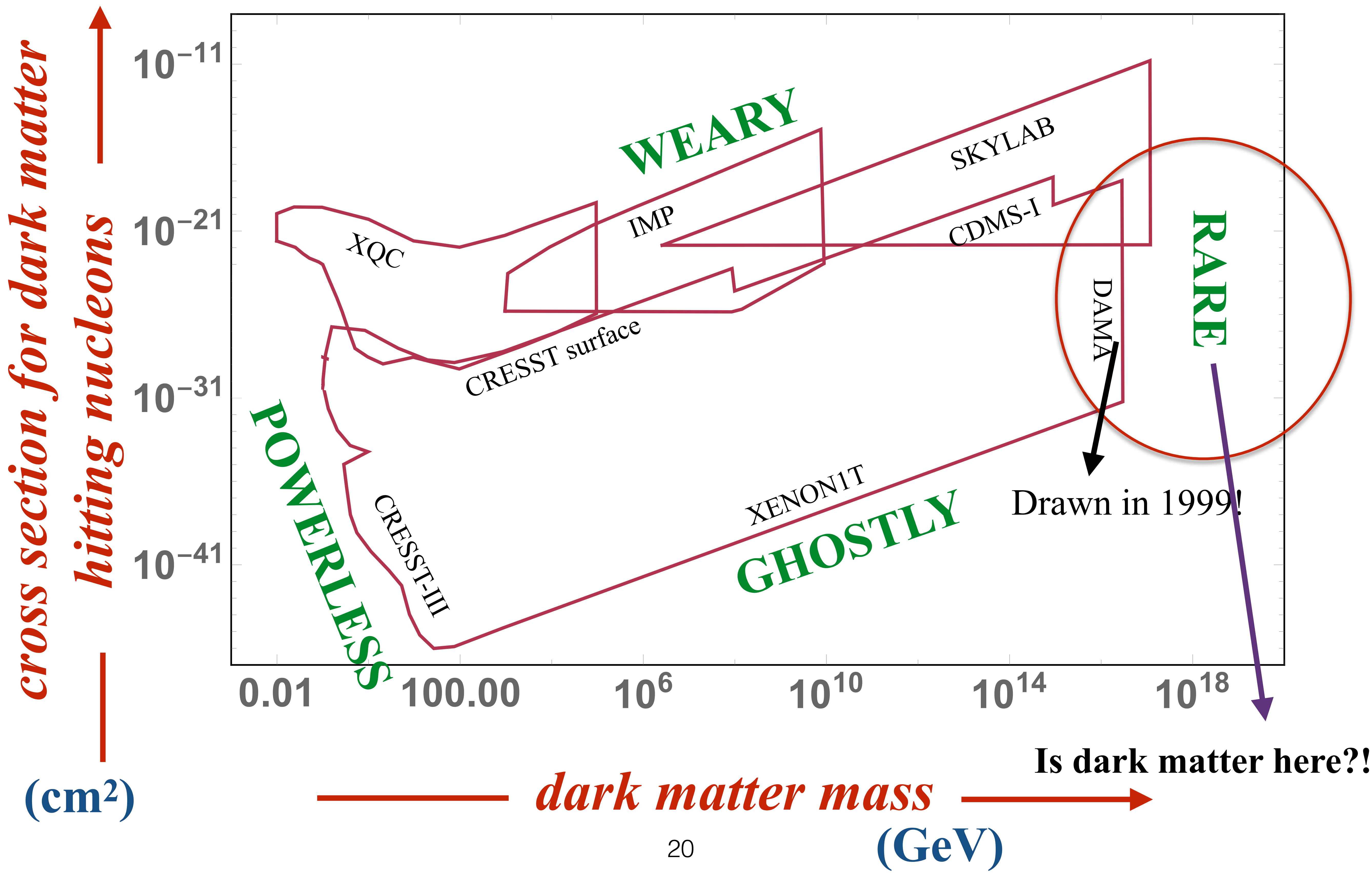

- Super-heavy states appear in theories of **grand unification of forces**.

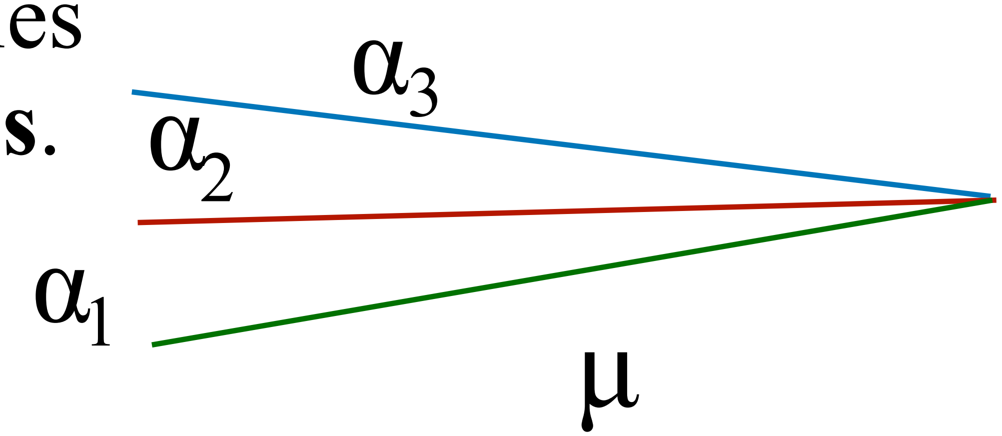

- Can make them in early universe:

  * Hawking radiation from primordial black holes
    Hooper, Krnjaic, McDermott (2019)

  * Gravitationally @ final stages of inflation
    Chung, Crotty, Kolb, Riotto (2001), Harigaya, Lin, Lou (2016)

  * Pre-heating: parametric resonance —> rapid decay of inflaton
    Giudice, Peloso, Riotto, Tkachev (1999), Bai, Korwar, Orlofsky (2020)

  * Thermally!
    Kim, Kuflik (2019)

Heavy, strong, stable: recent wave

Electroweak symmetric monopoles
Bai, Korwar, Orlofsky
2005.00503

Electroweak symmetric solitons
Bai, Jain, Ponton
1906.10739

Charged primordial black holes
Lehmann, Johnson, Profumo, Schwemberger
1906.06348

Asymmetric dark matter nuggets
Coskuner, Grabowska, Knapen, Zurek
1812.07573

Dark blobs
Grabowska, Melia, Rajendran
1807.03788

Colored relics
Gross, Mitridate, Redi, Smirnov, Strumia
1811.08418

Heavy dark baryons
Davoudiasl, Mohlabeng
1809.07768

Heavy dark skyrmions
Berezowski, Dick
Sep 2019

Why now?
Can detect them now!

Today's dark matter detectors

DAMA 1999 search

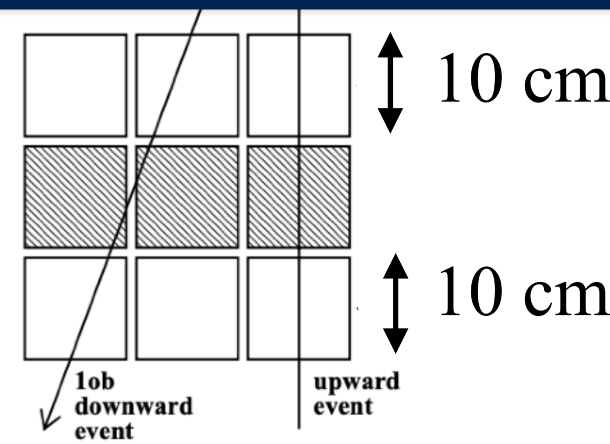

← 100 cm →

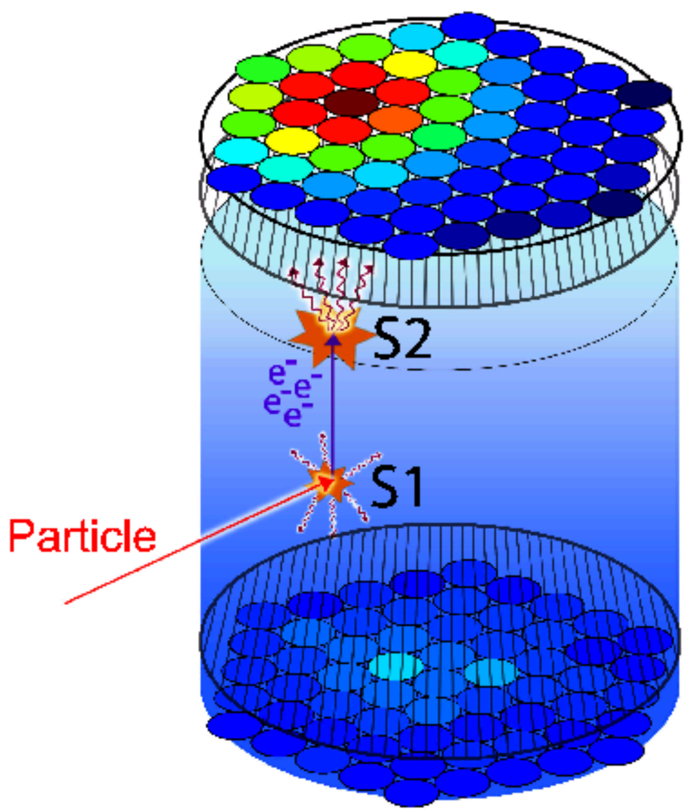

XENON1T/ LUX/ PANDAX-II

← 130 cm →

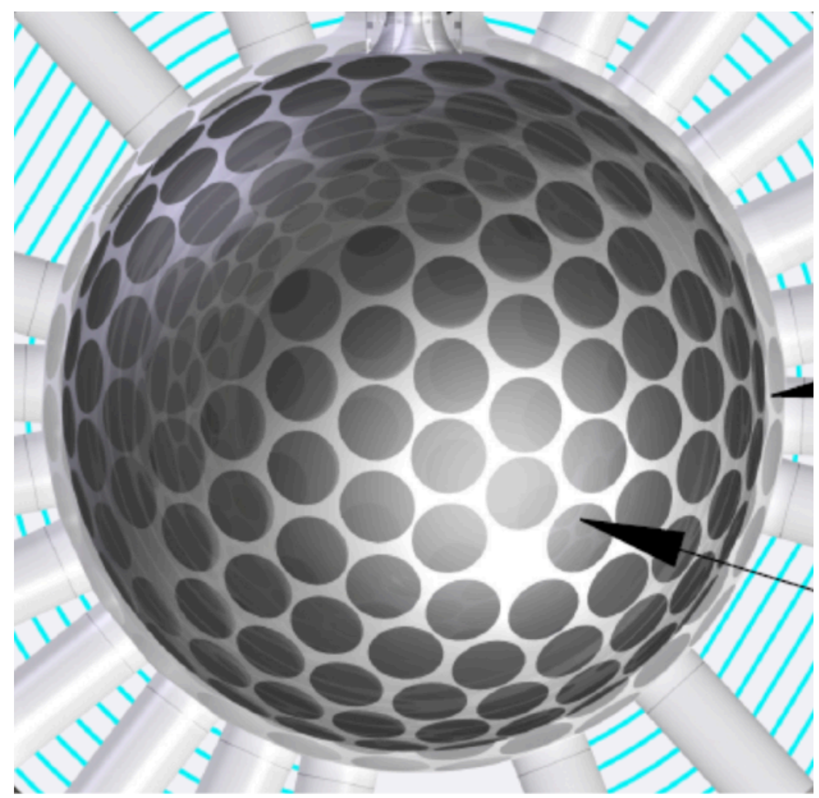

DEAP-3600

← 50 cm →

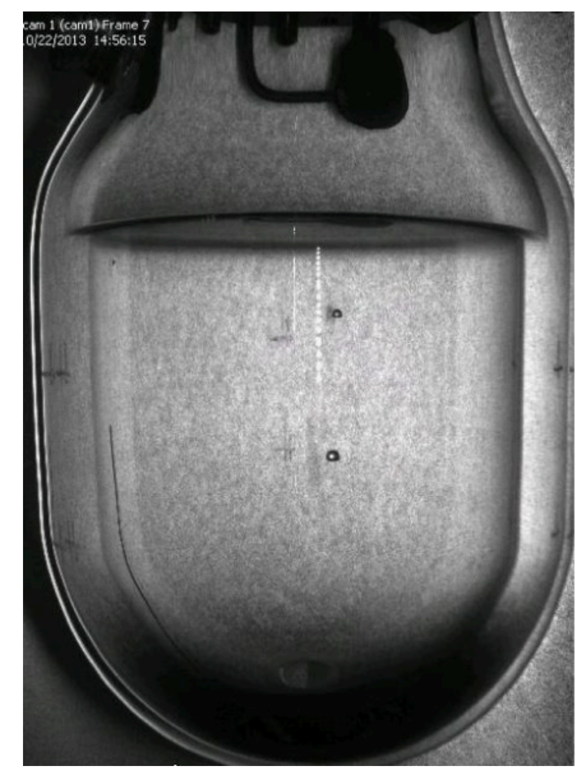

PICO-40L

Multiscatter signatures essential

 # scatters per transit = σ x target number density x path length

B. Broerman, J. Bramante, R. Lang, **N. Raj**
Phys.Rev.D. *(2018)*

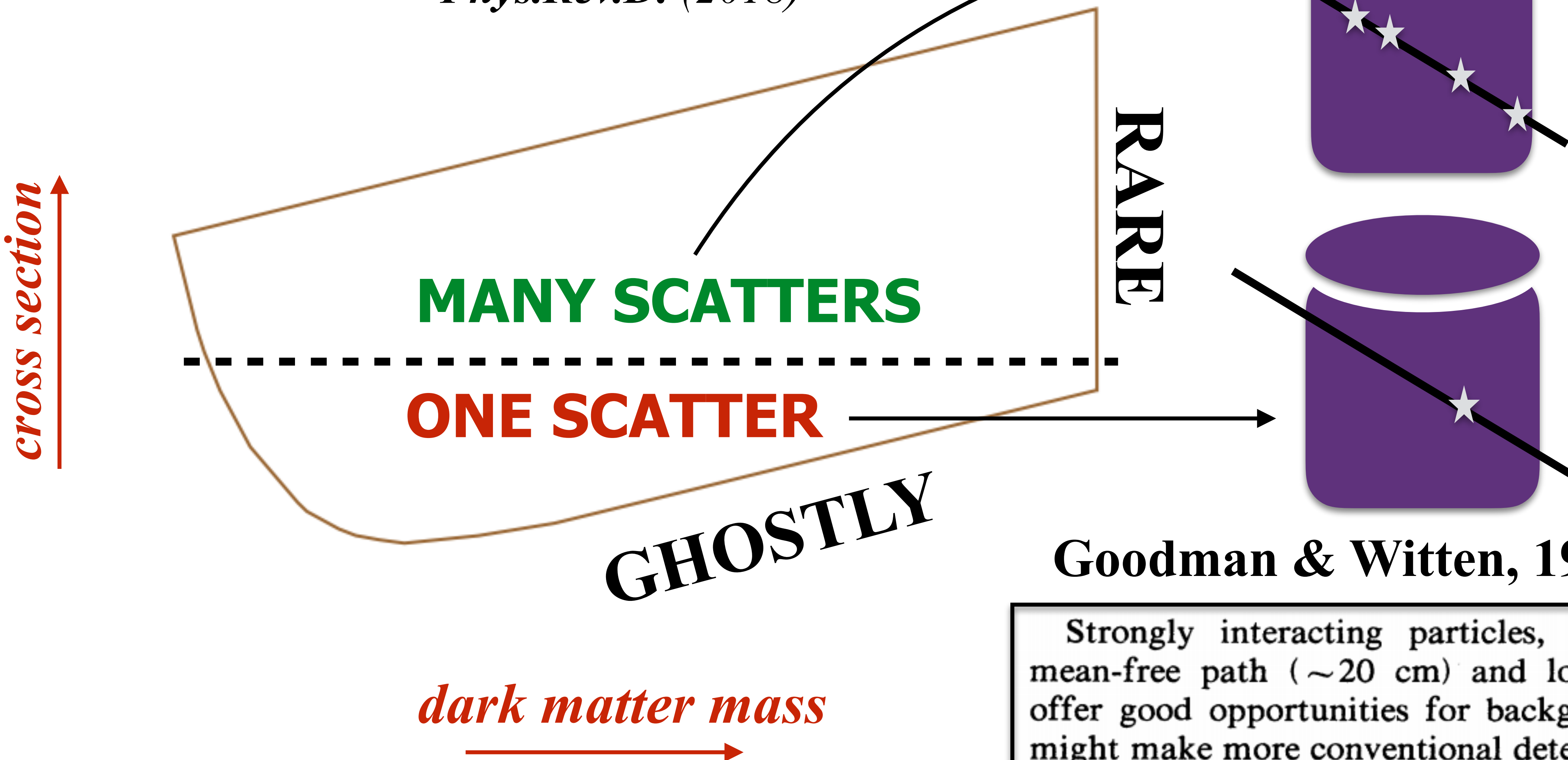

Goodman & Witten, 1985:

> Strongly interacting particles, with their observable mean-free path (~20 cm) and low velocity ($\beta \lesssim 10^{-3}$) offer good opportunities for background rejection which might make more conventional detection schemes feasible. A distinctive signal in a NaI crystal would be a pair of events with energy deposit ~10 keV (~10 photons detected) separated by ~20 cm and by ~1 μsec.

> a large range of masses for strongly interacting dark-matter particles is probably already ruled out by the simple observation that NaI does not "glow in the dark."

- DAMA '99 based on this 'multiple scatters' signature
- **Not** sought any more. Would double the reach of all current experiments!

DEAP-3600 @ SNOLAB

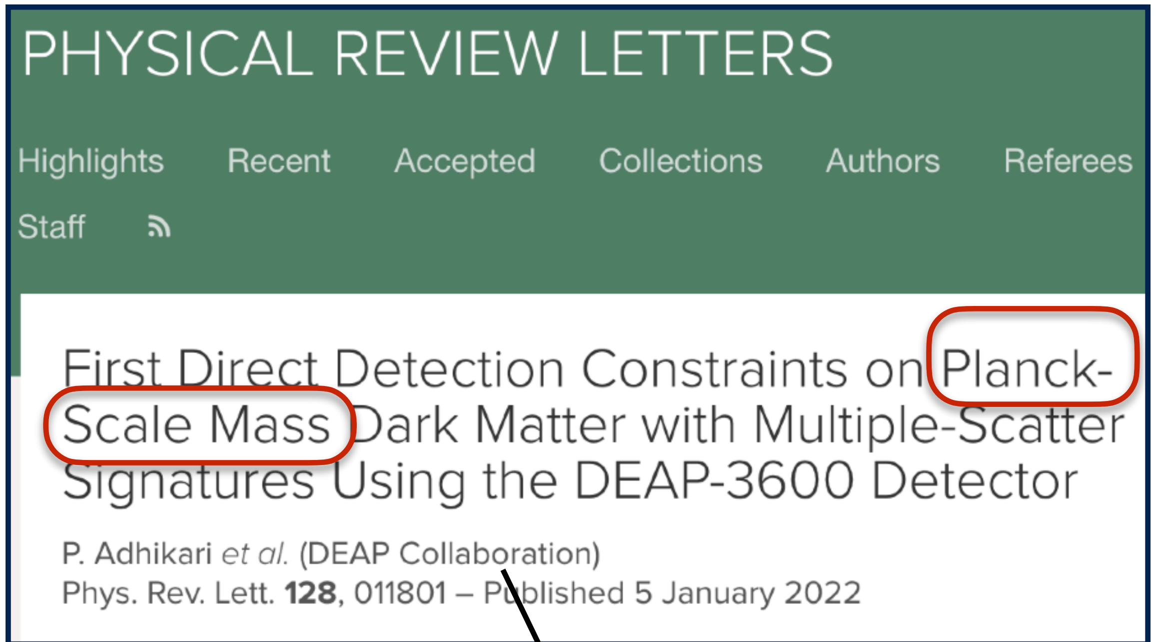
PHYSICAL REVIEW LETTERS

Highlights Recent Accepted Collections Authors Referees Staff

First Direct Detection Constraints on Planck-Scale Mass Dark Matter with Multiple-Scatter Signatures Using the DEAP-3600 Detector

P. Adhikari *et al.* (DEAP Collaboration)

Phys. Rev. Lett. **128**, 011801 – Published 5 January 2022

<u>working group</u>

W. Bonivento, S. Garg, M. Lai, **N. Raj**, *S. Westerdale.*

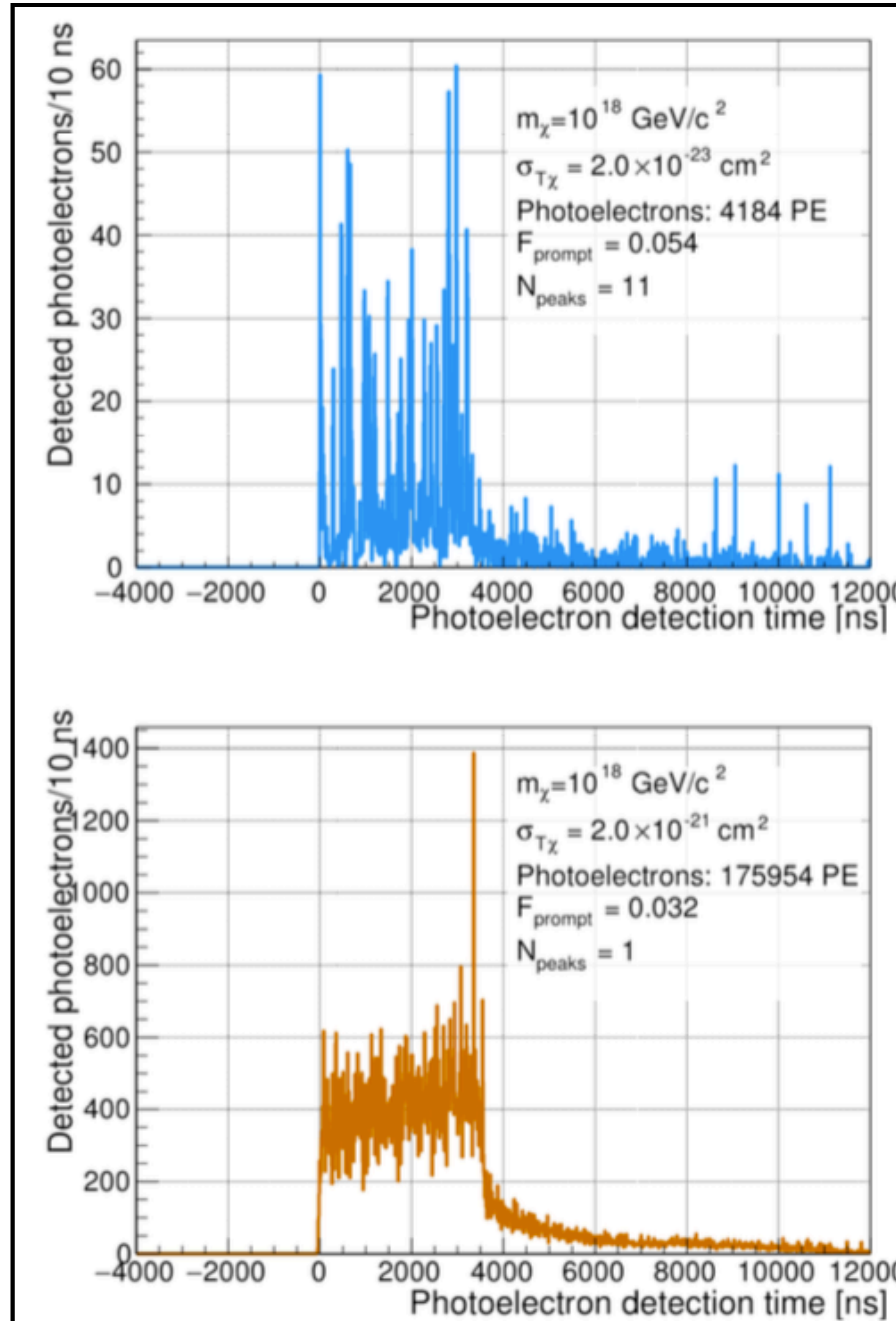

multiscatter signatures:

waveforms of energy deposition in liquid argon

Landscape of ultraheavy dark matter

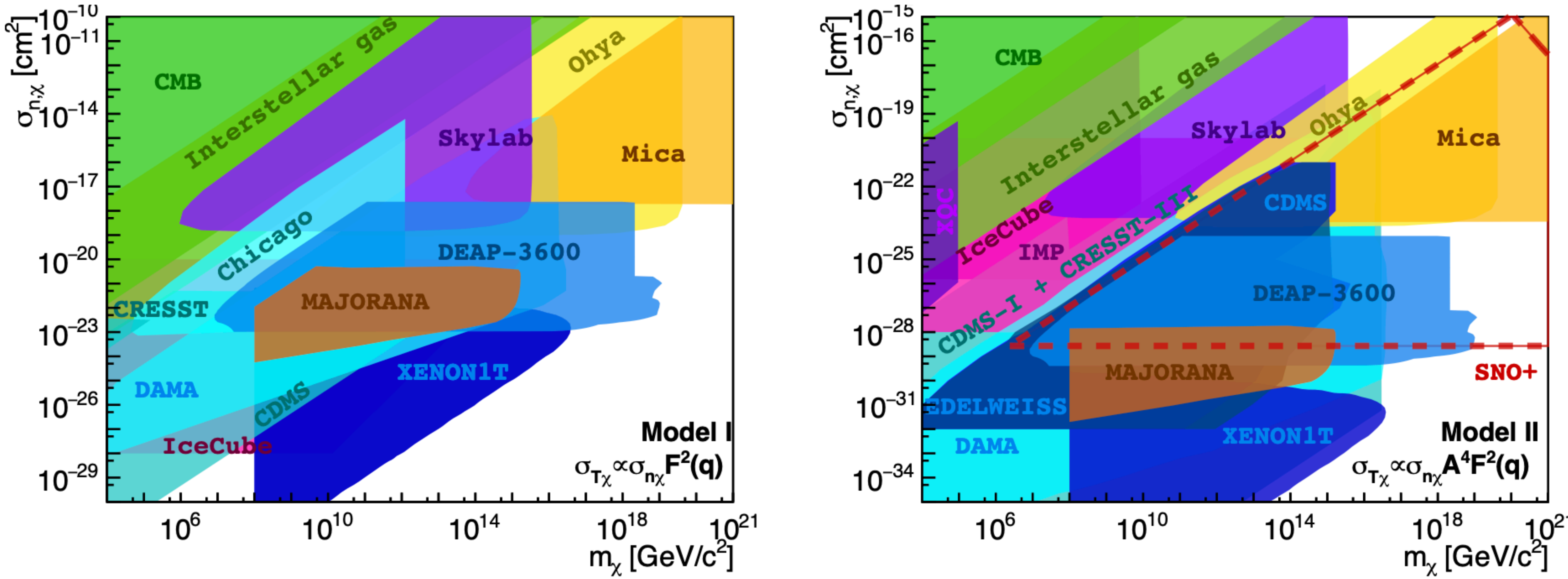

Snowmass whitepaper co-ordinated with Dan Carney; SciPost Phys Core 2023.

Preliminary

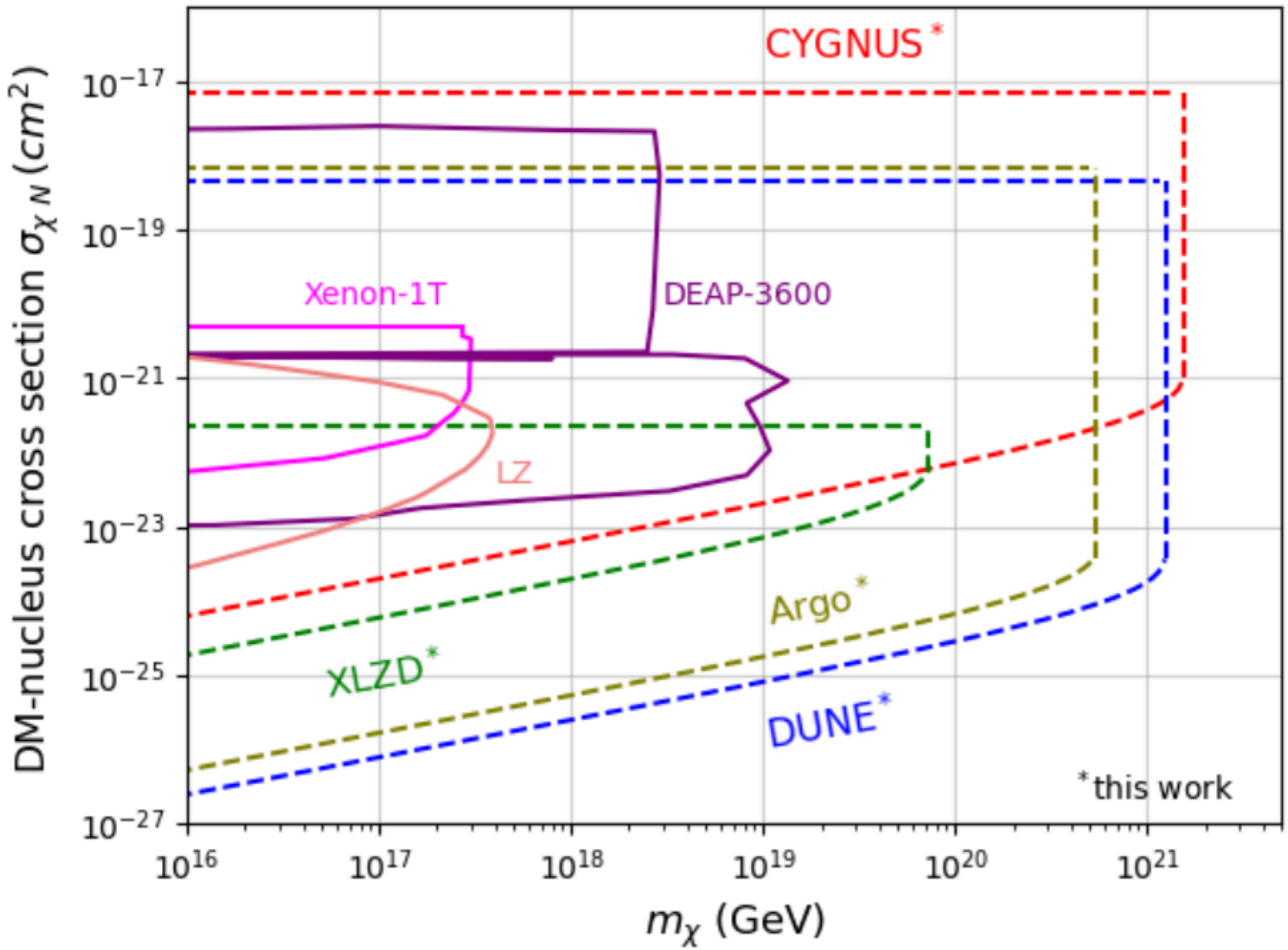

ongoing study with Harsh Aggarwal, IIT-KG

actual single-scatter ceiling
set by Poisson fluctuations
in hits-per-transit ("multiplicity")

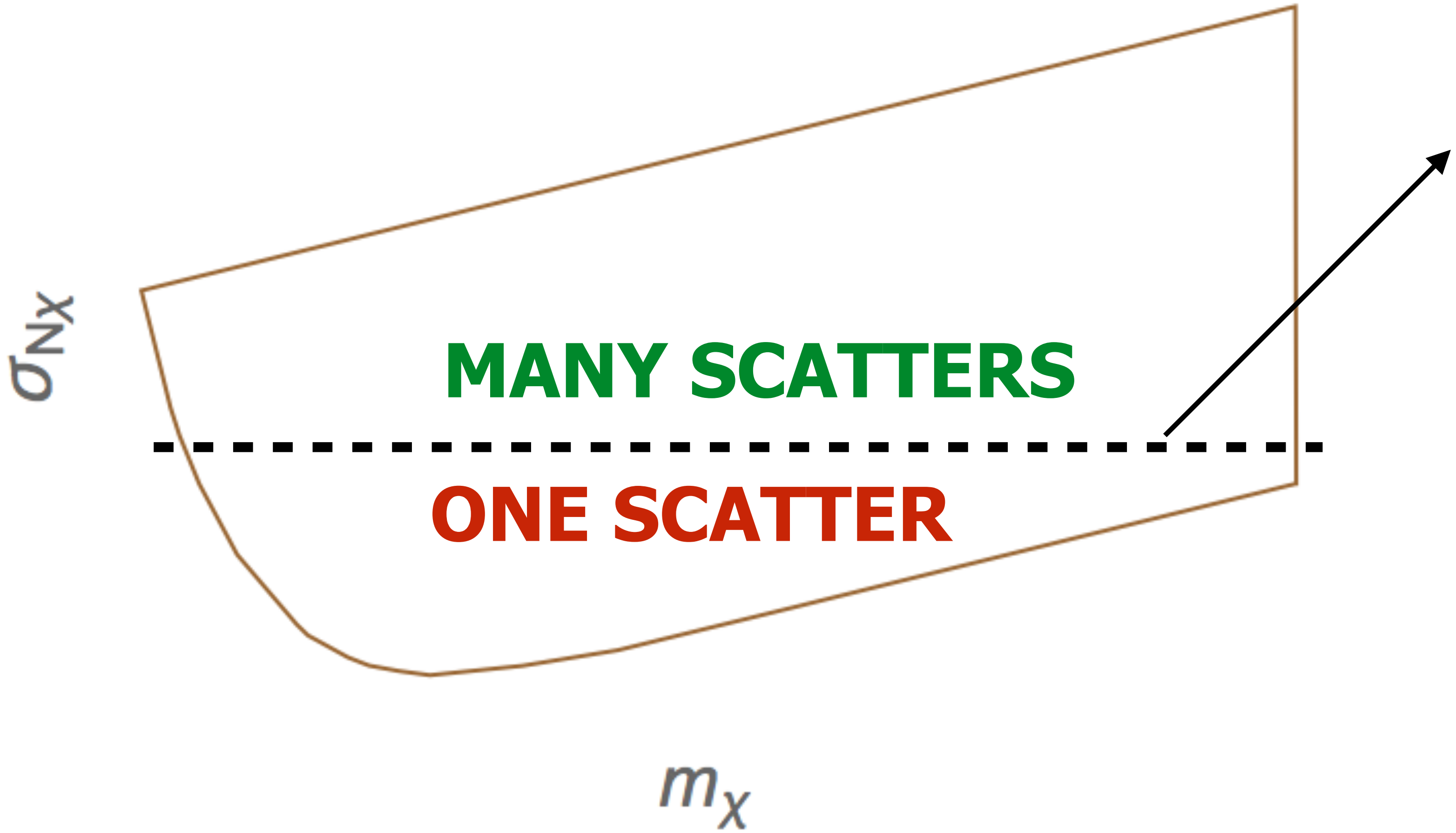

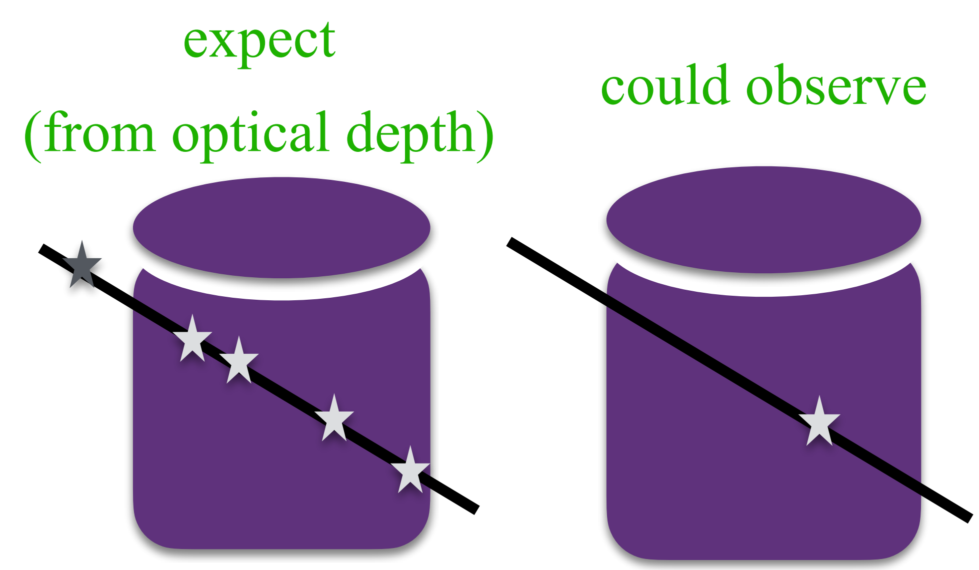

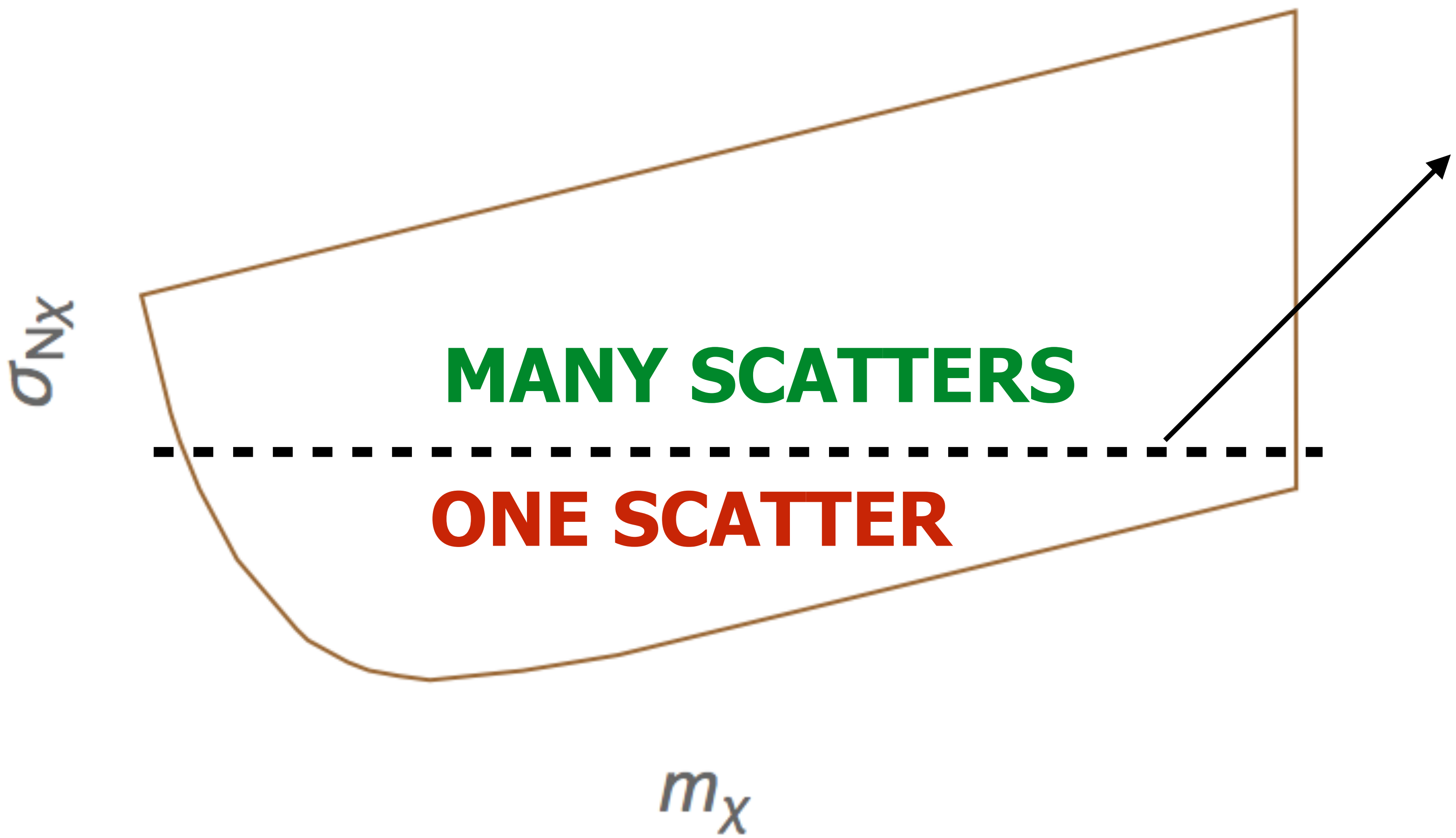

actual single-scatter ceiling
set by Poisson fluctuations
in hits-per-transit ("multiplicity")

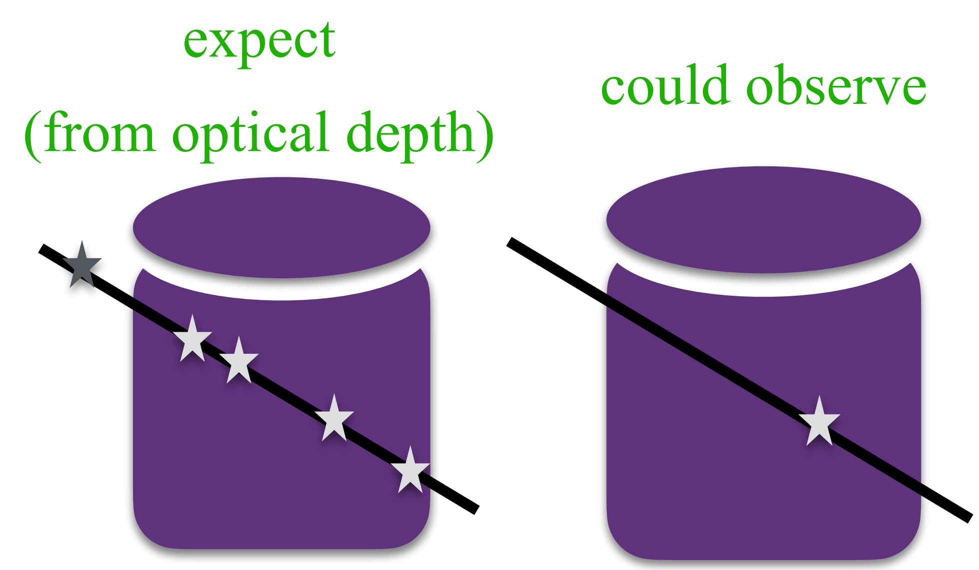

Why care?

(i) identify correctly where "WIMP" searches apply!

(ii) Poisson fluctuations => overlap with multi-scatter regions
=> cross-confirmation of search results

gets tricky & interesting in the presence of
(imminent) neutrino background!

At "ghostly frontier", problem already tackled: "*neutrino floor*"
by analogy, we have "*neutrino roof*"

“WIMP” event rate familiar from literature

$$\frac{dR}{dE_{\rm R}} = \left(\frac{\rho_\chi}{m_\chi}\right)\epsilon_{\rm NR}\int_{\rm v_{min}}^{v_{\rm esc}} d^3v\, v f_{\rm lab}(\vec{v})\frac{d\sigma_{\rm T\chi}}{dE_{\rm R}}\ ,$$

detection efficiency

$$\frac{d\sigma_{\rm T\chi}}{dE_{\rm R}} = \frac{m_{\rm T}}{2\mu_{\rm T\chi}^2 v^2}\sigma_{\rm T\chi}S(E_{\rm R})$$

structure factor

....

“WIMP” event rate familiar from literature

$$\frac{dR}{dE_{\rm R}} = \left(\frac{\rho_\chi}{m_\chi}\right)\epsilon_{\rm NR}\int_{v_{\rm min}}^{v_{\rm esc}} d^3v\, v f_{\rm lab}(\vec{v})\frac{d\sigma_{{\rm T}\chi}}{dE_{\rm R}}\,,$$

$$\frac{d\sigma_{{\rm T}\chi}}{dE_{\rm R}} = \frac{m_{\rm T}}{2\mu_{{\rm T}\chi}^2 v^2}\sigma_{{\rm T}\chi}S(E_{\rm R})$$

detection efficiency

structure factor

$N_{\rm hit}^{\rm exp} \ll 1$

our generalization

$$N_{\rm ev}^{\rm SS} = \epsilon_{\rm NR}\; p_{\rm hit}(1, N_{\rm hit}^{\rm exp}) \left(\frac{\rho_\chi}{m_\chi}\right)\pi R_{\rm fid}^2 \bar{v} t_{\rm exp}$$

“multiplicity”/ optical depth: $\sigma_{{\rm T}\chi}^{\rm eff} n_{\rm T} L_{\rm ave}$

$$p_{\rm hit}(k,\lambda) = \frac{\lambda^k e^{-\lambda}}{k!}$$

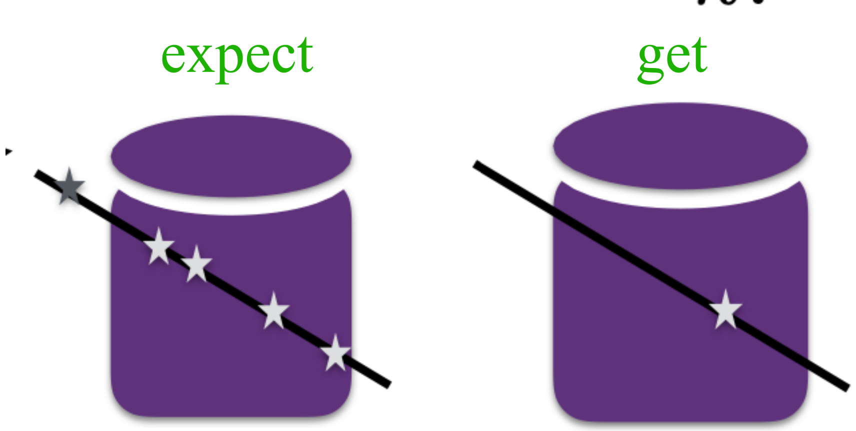

detectable total cross section:

$$\sigma_{{\rm T}\chi}\frac{m_{\rm T}}{2\mu_{{\rm T}\chi}^2\bar{v}}\int_{E_{\rm R,min}}^{E_{\rm R,max}} dE_{\rm R}\, S(E_{\rm R})\eta(E_{\rm R})$$

usual “velocity integral”

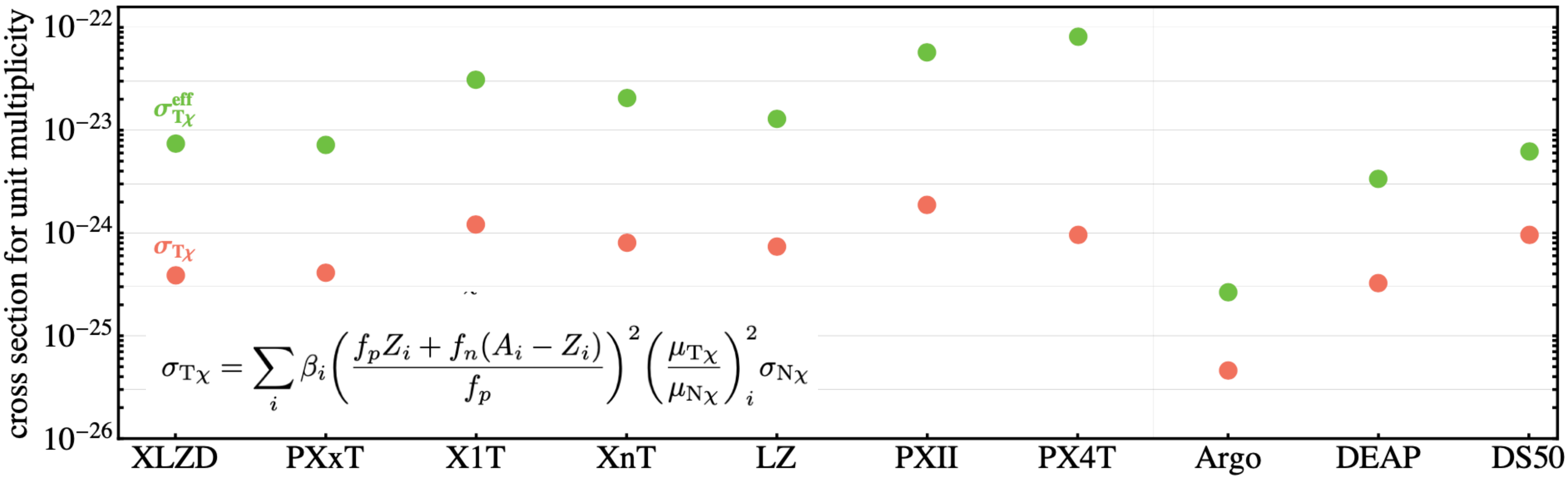

target	detector	$M_{\rm fid} \times t_{\rm exp}$ (ton × yr)	$E_{\rm R}$ (keV)	$\epsilon_{\rm NR}$	$(N_{\rm B} \pm \sigma_B,\ N_{\rm obs}, N^{\rm 90CL}_{\rm exp})$
xenon 2.94 g/cm^3 ^{128}1.9%, $^{129}_{\rm SD}$26.4%, ^{130}4.1% $^{131}_{\rm SD}$21.2%, ^{132}26.9%, ^{134}10.4%, ^{136}8.9%	**DARWIN/XLZD** [21]	40 × 5	[5, 35]	0.50	(4.1, 4.1, 4.0)
	PANDAX-xT [23]	34.2 × 5.85	[4, 35]	0.50	(48±6.9, 48, 11.4)
	XENON1T [19]	1.3 × 0.76	[10, 40]	0.80	(7.4±0.6, 14, 12.8)
	XENONnT [34]	4.18 × 0.26	[10, 40]	0.80	(2.03±0.16, 3, 4.7)
	LZ [35]	5.5 × 0.16	[5, 50]	0.90	(–,–, 4.4)
	PANDAX-II [36]	0.33 × 1.1	[10, 30]	0.85	(40.3±3.1, 38, 7.8)
	PANDAX-4T [37]	2.67 × 0.24	[30, 90]	0.75	(9.8±0.6, 6, 0.8)
	KILOXENON	40 × 25	[5, 35]	0.50	$(20.6{\pm}6.1, 20.6^{\times 2}_{\div 2}, 10.9^{+6.3}_{-6.7})$
	MYRIAXENON	10^3 × 10 ✶	[5, 35]	0.50	$(206{\pm}44, 206^{\times 2}_{\div 2}, 60^{+44}_{-45})$
argon 1.40 g/cm^3 ^{36}0.33%, ^{38}0.06%, ^{40}99.6%	**DarkSide-20k** [24]	20 × 10	[30, 200]	0.90	(3.2, 3.2, 3.7)
	Argo [25]	300 × 10	[55, 100]	0.90	(15.6±5, 15.6, 6.4)
	DarkSide-50 [38]	0.031 × 1.46	[80, 200]	0.70	(0, 0, 2.3)
	DEAP-3600 [39]	0.824 × 0.63	[70, 100]	0.24	(0, 0, 2.3)
	MYRIARGON	300 × 33.3	[55, 100]	0.90	$(51.5{\pm}12.6, 51.5^{\times 2}_{\div 2}, 19.7^{+13.1}_{-13.2})$
	DECIMEGARGON	10^4 × 10 ✶	[55, 100]	0.90	$(515{\pm}106, 515^{\times 2}_{\div 2}, 174^{+106}_{-106})$

✶ noble detector masses motivated by $0\nu\beta\beta$-driven research & DUNE: see 2404.19050, 2301.11878, ...

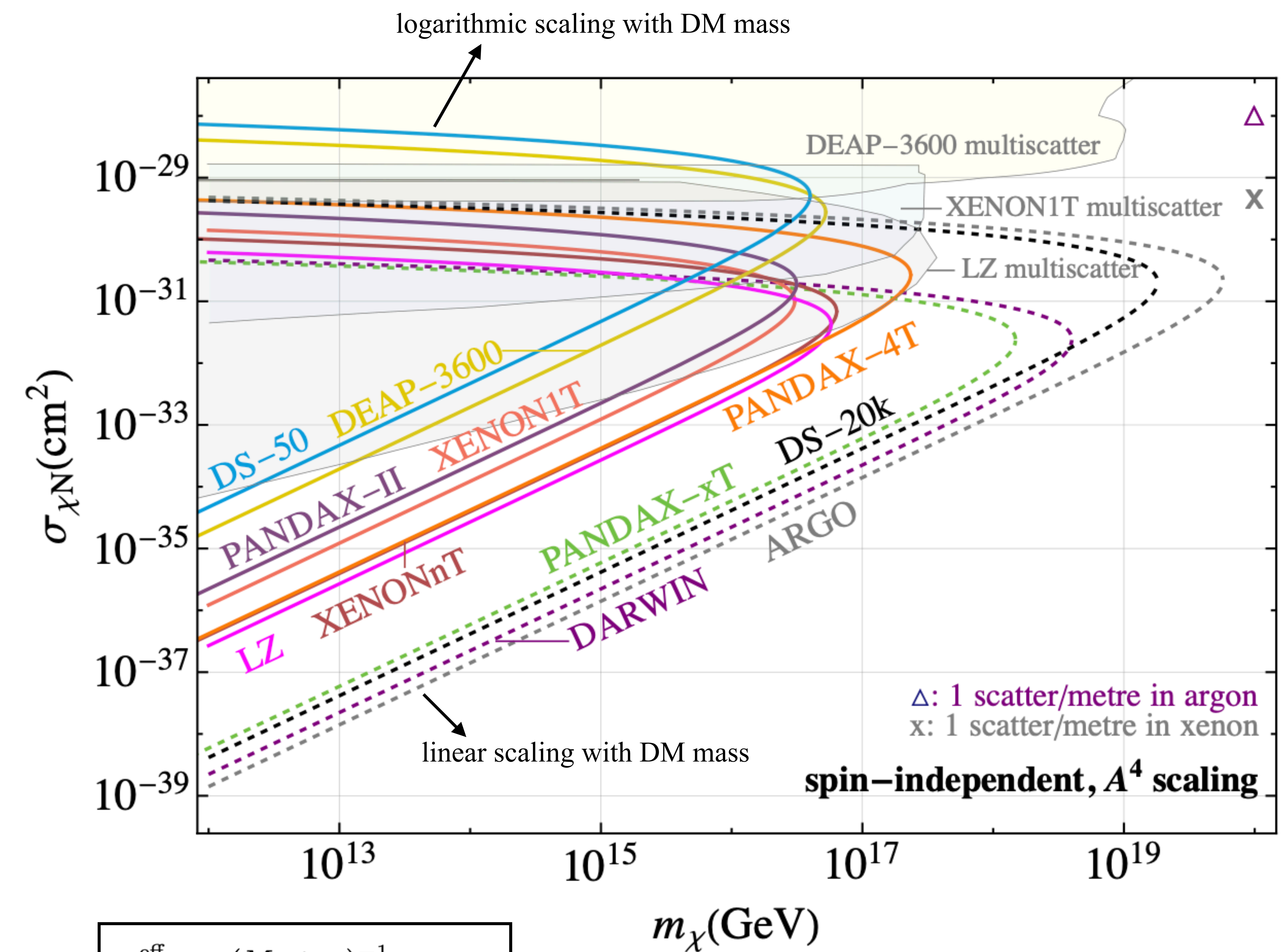

floor $\quad {}_b\sigma^{\mathrm{eff}}_{\mathrm{T}\chi} \propto (M_{\mathrm{fid}} t_{\mathrm{exp}})^{-1}$,

ceiling $\quad {}_t\sigma^{\mathrm{eff}}_{\mathrm{T}\chi} \propto M_{\mathrm{fid}}^{-1/3} \log(M_{\mathrm{fid}}^{2/3} t_{\mathrm{exp}})$

Raj & Mondal, 2406.17015

Xe-phobic floors good news for argon experiments

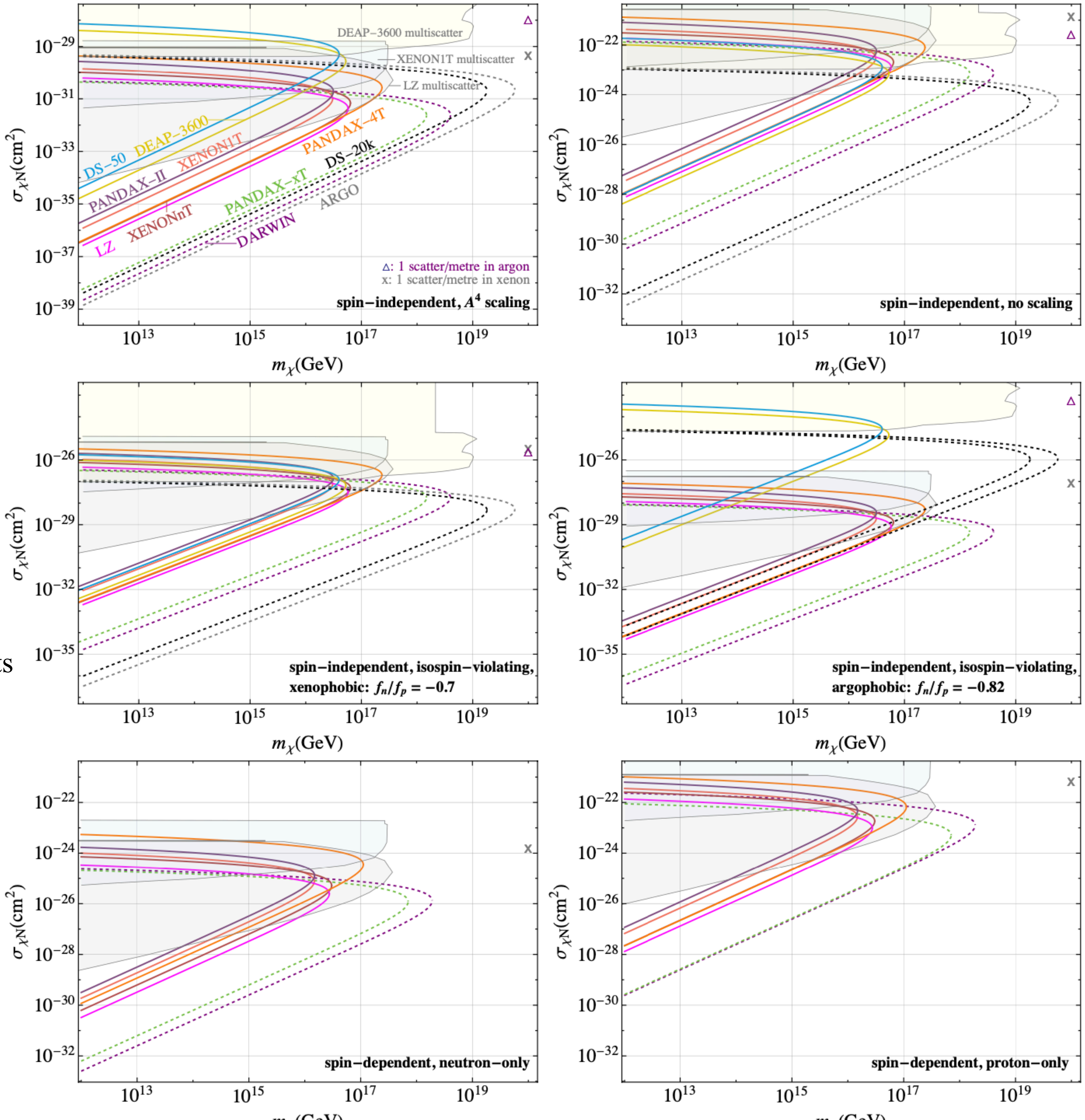

Ar-phobic roofs good news for argon experiments

Raj & Mondal, 2406.17015

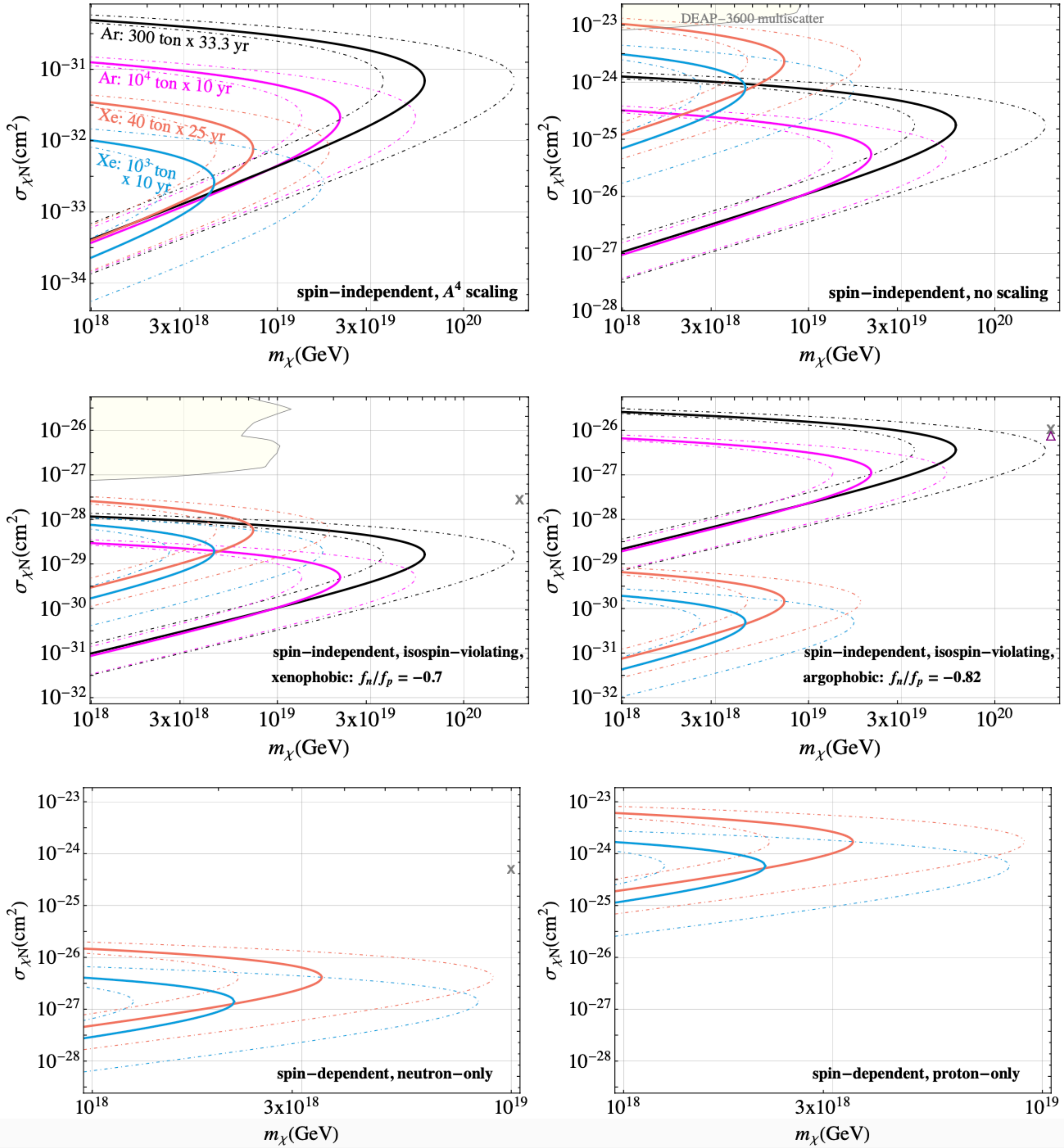

Raj & Mondal, 2406.17015

Conclusion

Ceilings are as important as floors!

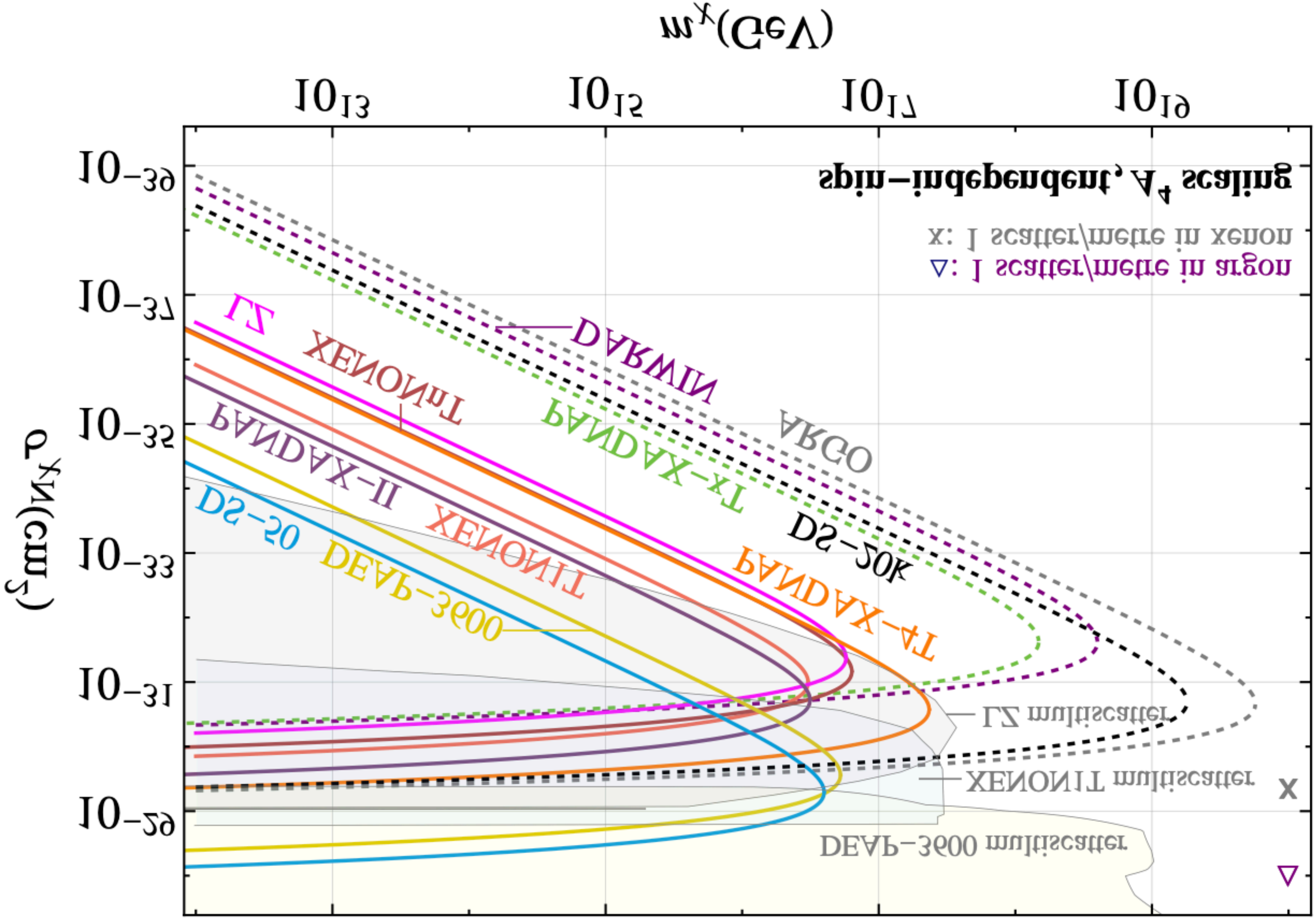

🙏

?

recasting

MAJORANA DEMONSTRATOR

search for lightly ionizing particles

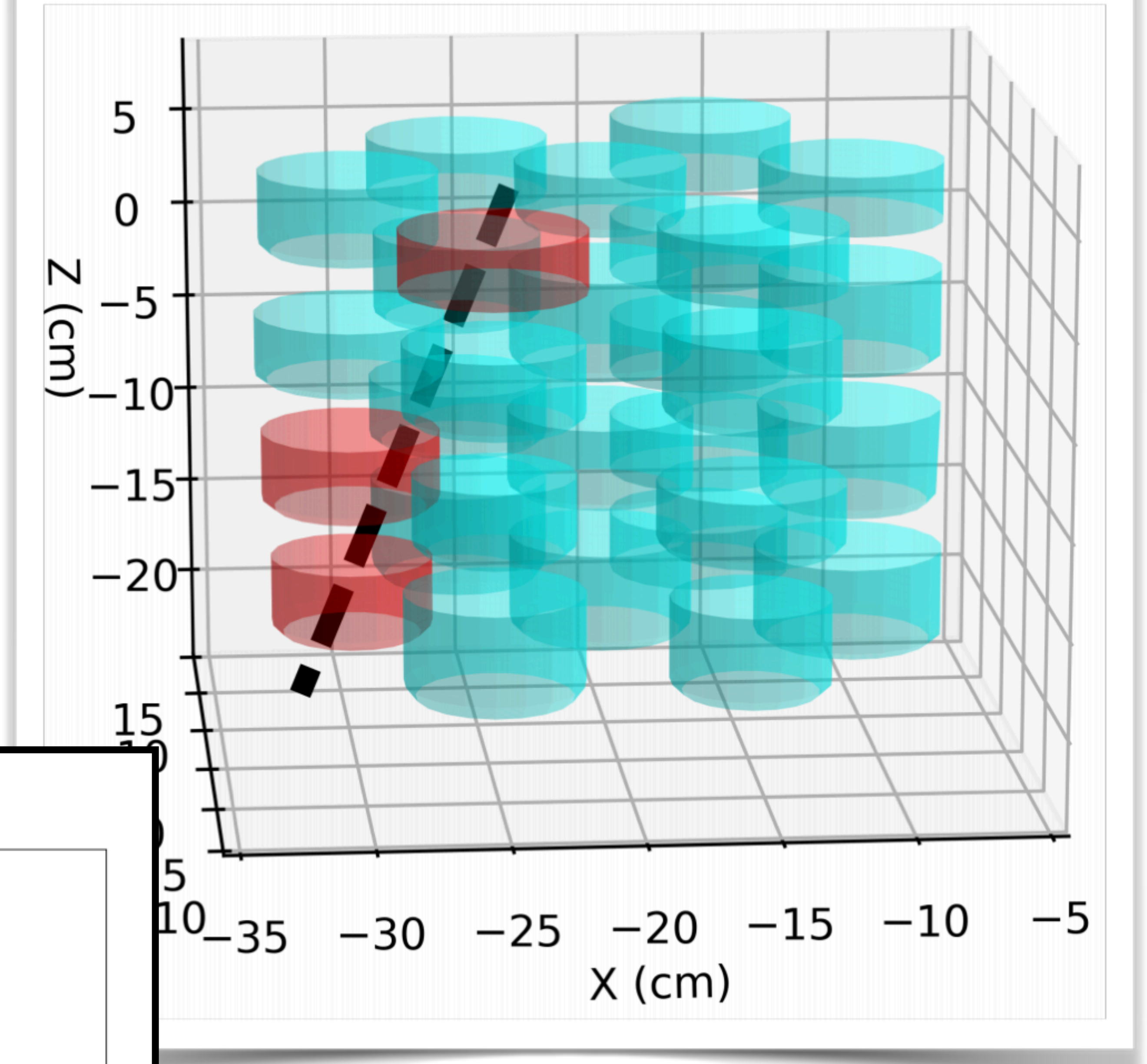

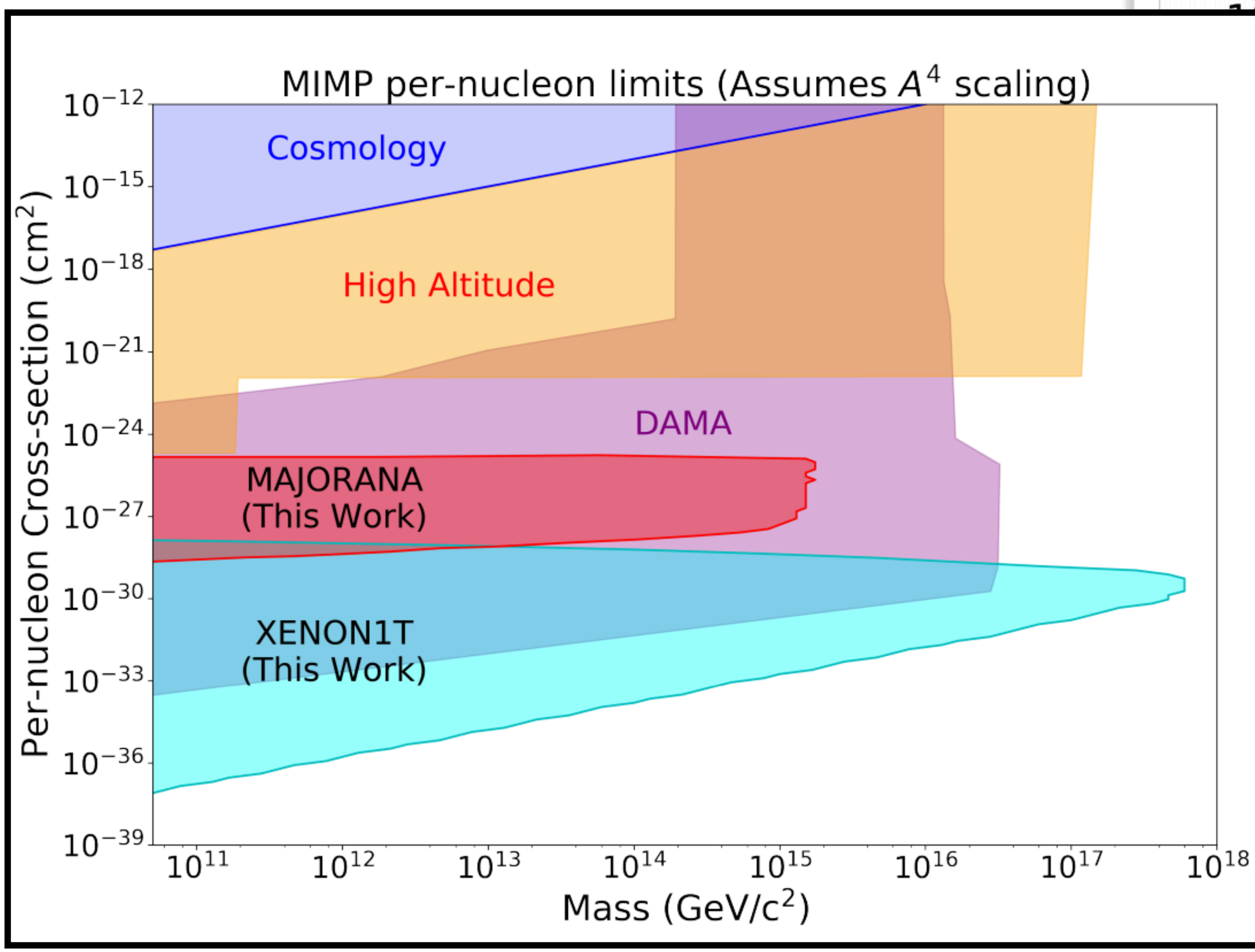

‘Direct Detection Limits on Heavy Dark Matter’

2009.07909

M. Clark, R. Lang et al

(Q1) Identifying multiscatterers

DM transit = 2.5 μs

	LUX/PANDAX/XENON1T	PICO-60
WIMP:	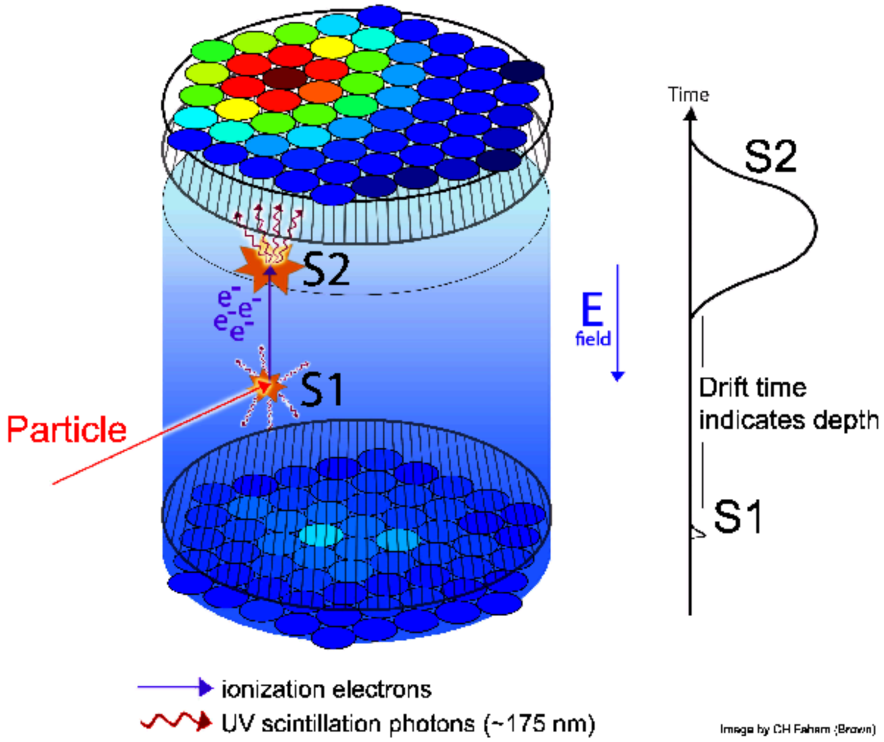	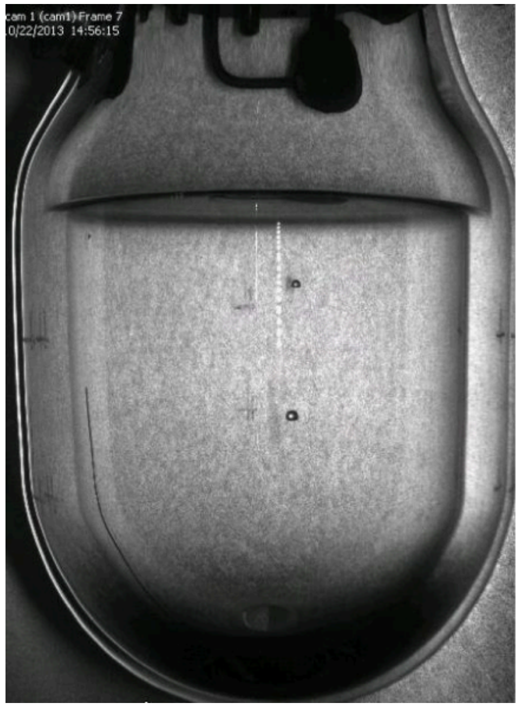
MIMP:	Train of scintillation pulses + electroluminescence pulses For multiplicity > 5 (>500), S2 (S1) pulses merge into elongated pulses	Track of bubbles Stereo cameras can image up to 100 bubbles (mm resolution)

- Background ~ 0 (from daughter neutrons of surrounding material & coincident electron recoils)

(Q1) Going to the Planck mass

DEAP-3600 @ SNOLAB

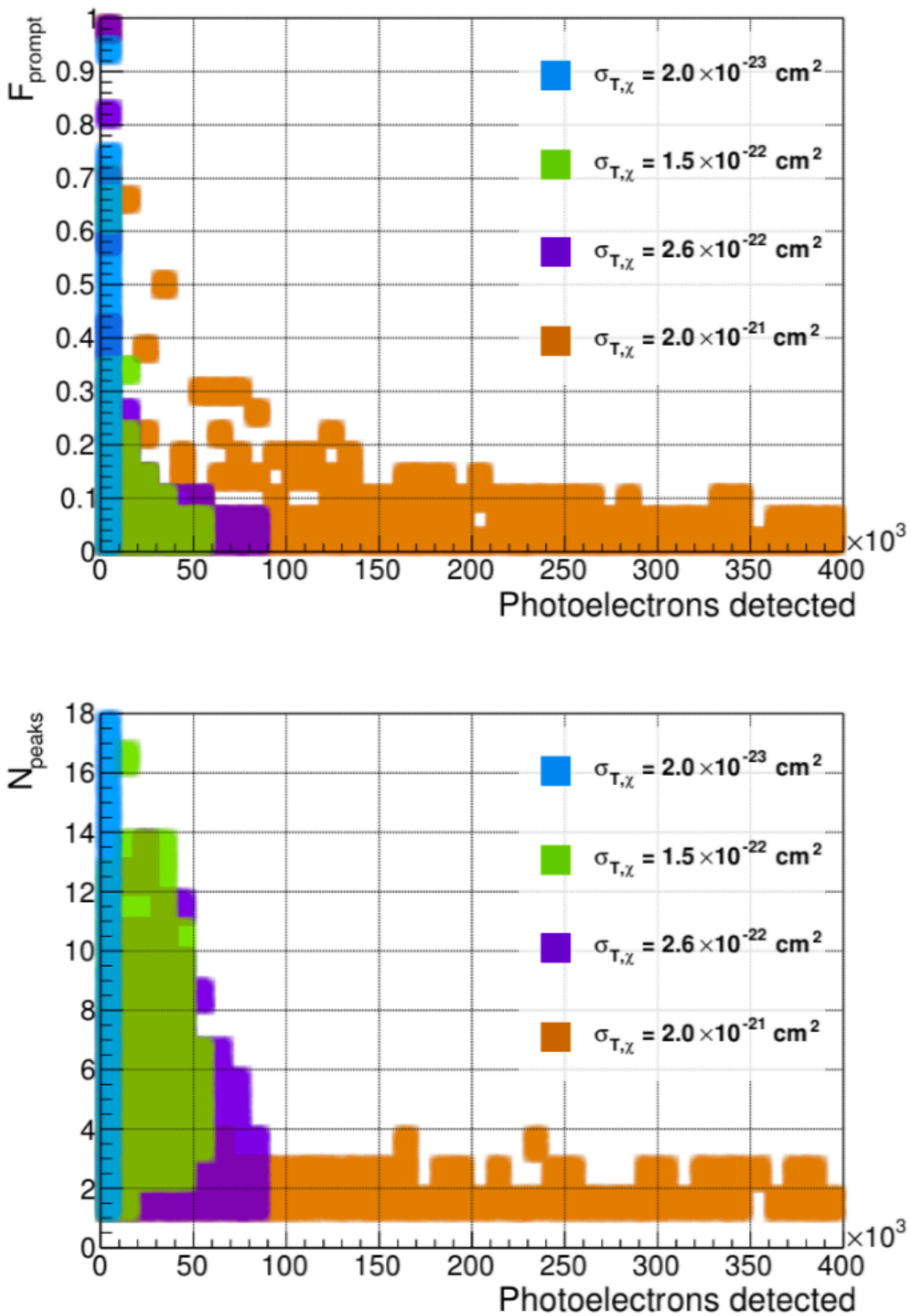

FIG. 2. Simulated F_{prompt} and N_{peaks} distributions for DM with $m_\chi = 10^{18}$ GeV/c^2 for various $\sigma_{T\chi}$.

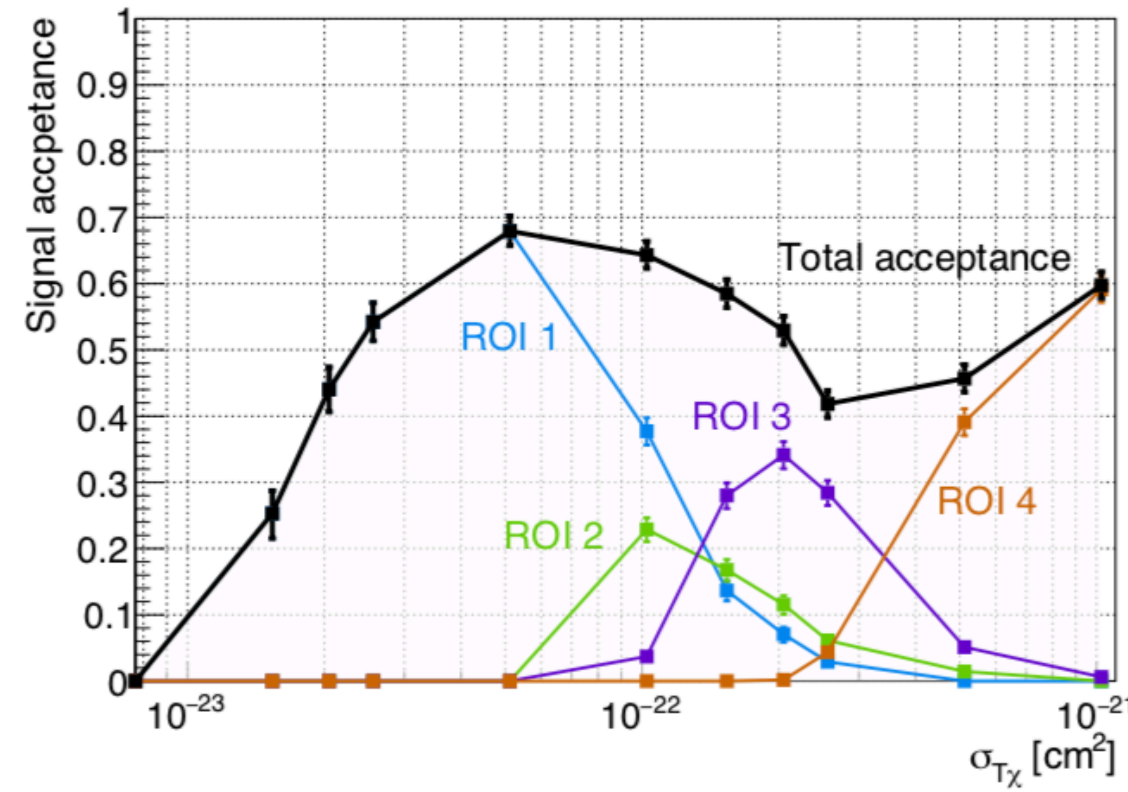

FIG. 3. Probability of DM with $m_\chi = 10^{18}$ GeV/c^2 populating each ROI and surviving all cuts at varying $\sigma_{T\chi}$.

ROI	PE range	Energy [MeV]	N_{peaks}^{min}	F_{prompt}^{max}	μ_b	$N_{obs.}$
1	4000–20 000	0.5–2.9	7	0.10	$(4 \pm 3) \times 10^{-2}$	0
2	20 000–30 000	2.9–4.4	5	0.10	$(6 \pm 1) \times 10^{-4}$	0
3	30 000–70 000	4.4–10.4	4	0.10	$(6 \pm 2) \times 10^{-4}$	0
4	70 000–4×10^8	10.4–60 000	0	0.05	$(10 \pm 3) \times 10^{-3}$	0

Reconstructing dark matter velocity vector

Image: Borexino 1308.0443

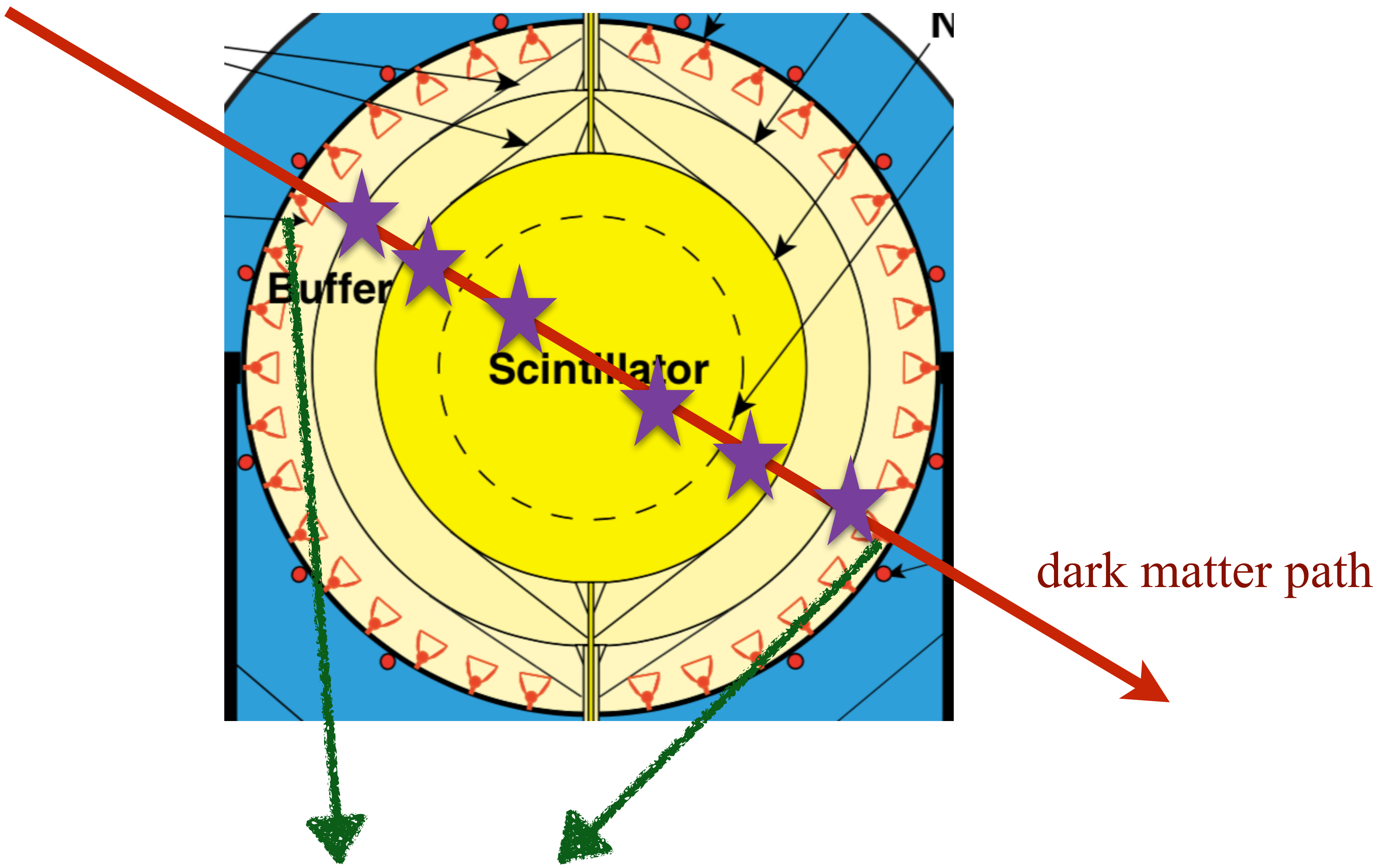

PMT "hot spots"
with numerous illuminations
=> **dark matter direction & path length**
+ timestamps
=> **dark matter speed**

J. Bramante, J. Kumar, **N. Raj**
Phys Rev D **(2019)**

Detector resolutions

J. Bramante, J. Kumar, **N. Raj**
***Phys Rev D* (2019)**

$$\delta\psi \simeq \frac{\Delta d}{L}$$ (PMT spacing/ path length)

Variable uncertainty	Baseline resolution
angle: $\delta\psi$	$\mathbf{3.7 \times 10^{-2}}$

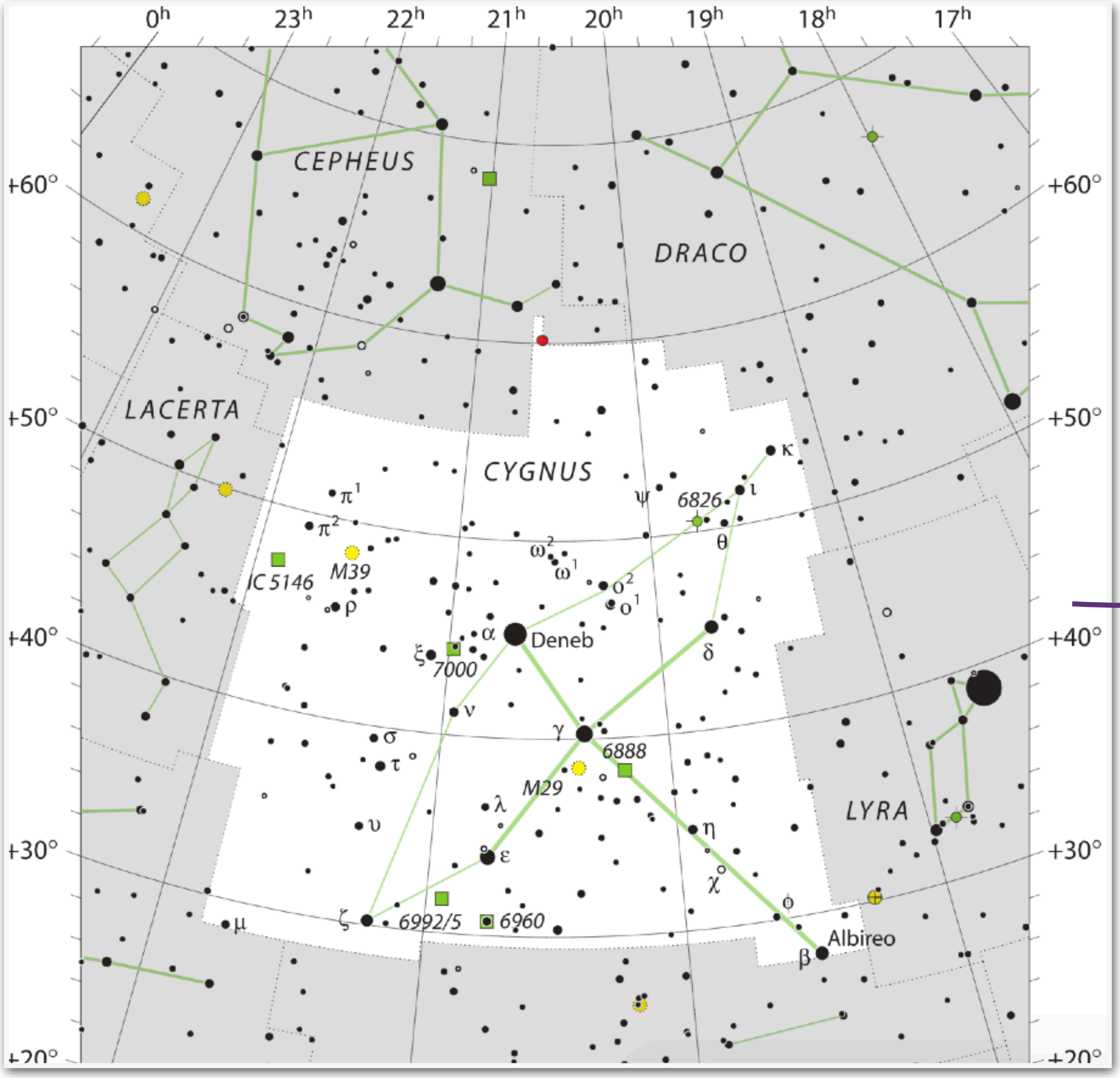

~2 degrees, c.f. Cygnus spanning > 20 degrees

Detector resolutions

J. Bramante, J. Kumar, **N. Raj**
***Phys Rev D* (2019)**

$$\delta\psi \simeq \frac{\Delta d}{L}$$ (PMT spacing/ path length)

$(\delta\psi)^2/2$

Variable uncertainty	Baseline resolution
angle: $\delta\psi$	$\mathbf{3.7 \times 10^{-2}}$
longitudinal path length: $\delta L/L$	6.7×10^{-4}
timing: $\delta T/T$	10^{-4}
speed: $\delta \mathbf{v}/\mathbf{v}$	$\mathbf{6.7 \times 10^{-4}}$

(< 1 km/s)

detector timing resolution

$$\frac{\delta v}{v} = \sqrt{\left(\frac{\delta L}{L}\right)^2 + \left(\frac{\delta T}{T}\right)^2}$$

detector uncertainties tiny => smearing negligible => main limitation is statistics!
(triumph of experimental progress)

Statistics

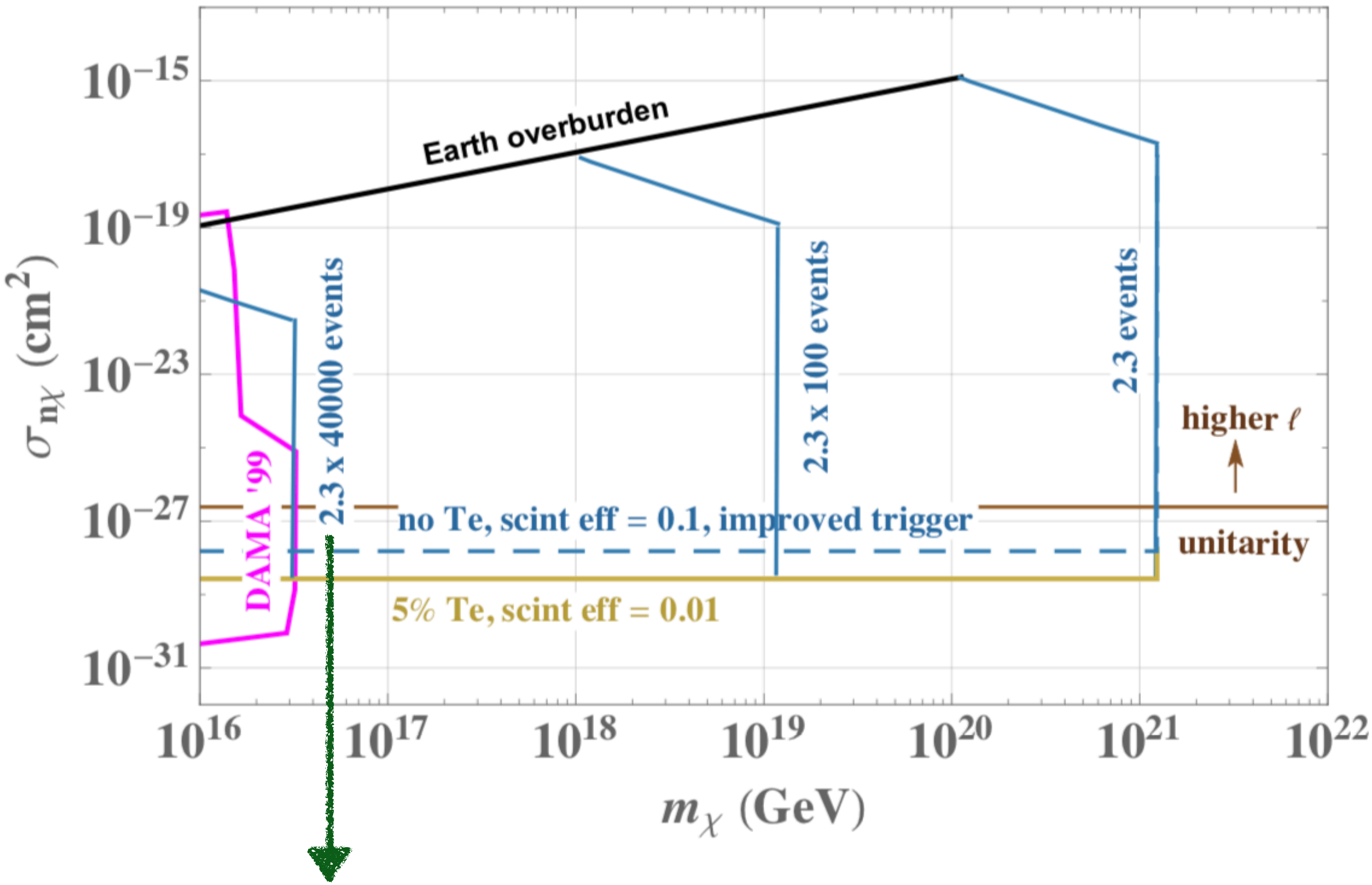

SNO+ could potentially collect these many events

J. Bramante, J. Kumar, **N. Raj**
***Phys Rev D* (2019)**

different scalings with detector mass & exposure

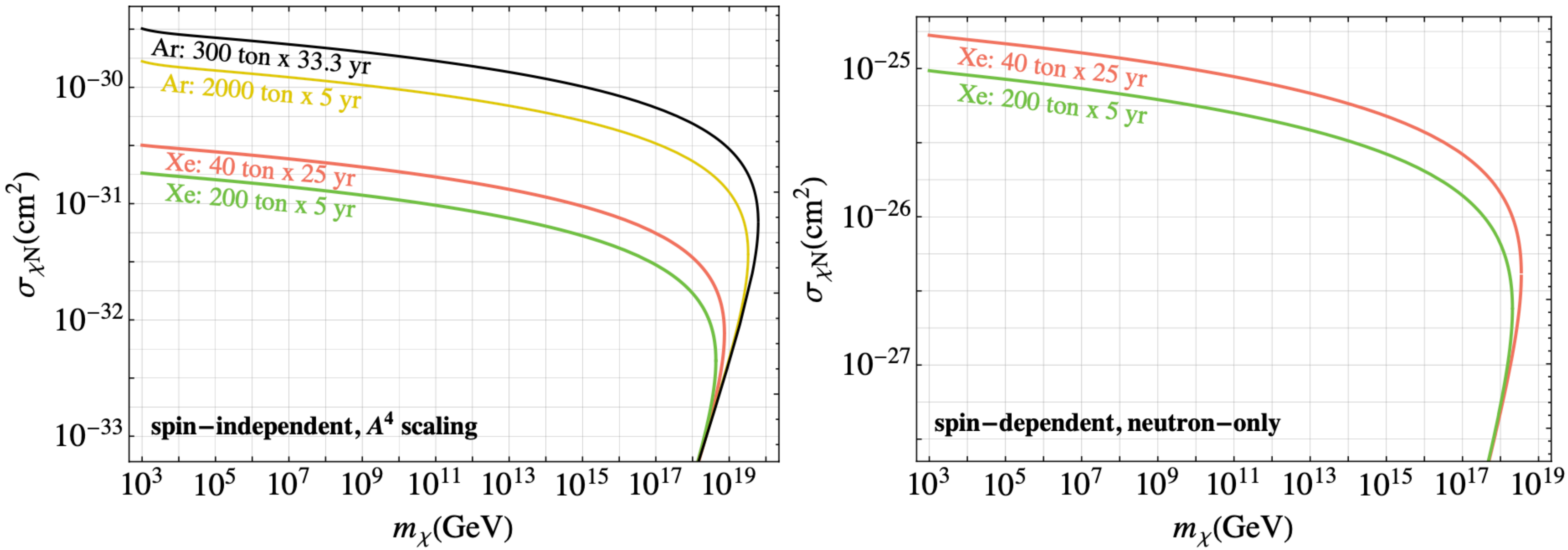

Raj & Mondal, 2406.17015

Dark astrometry

reconstruct velocity vector event-by-event

↓

assemble distributions of speed and angle

↓

determine **halo properties!**

dispersion speed | **escape speed** | **anisotropies**

+

bonus: **reject backgrounds**

J. Bramante, J. Kumar, **N. Raj**

***Phys Rev D* (2019)**

Pinpointing mean speed

galactic frame

$$f(v) = \frac{1}{\mathcal{N}} v^2 \exp\left(-\frac{v^2}{v_0^2}\right) \Theta(v_{\rm esc} - v)$$

v_0 = circular speed = √(2/3) dispersion speed

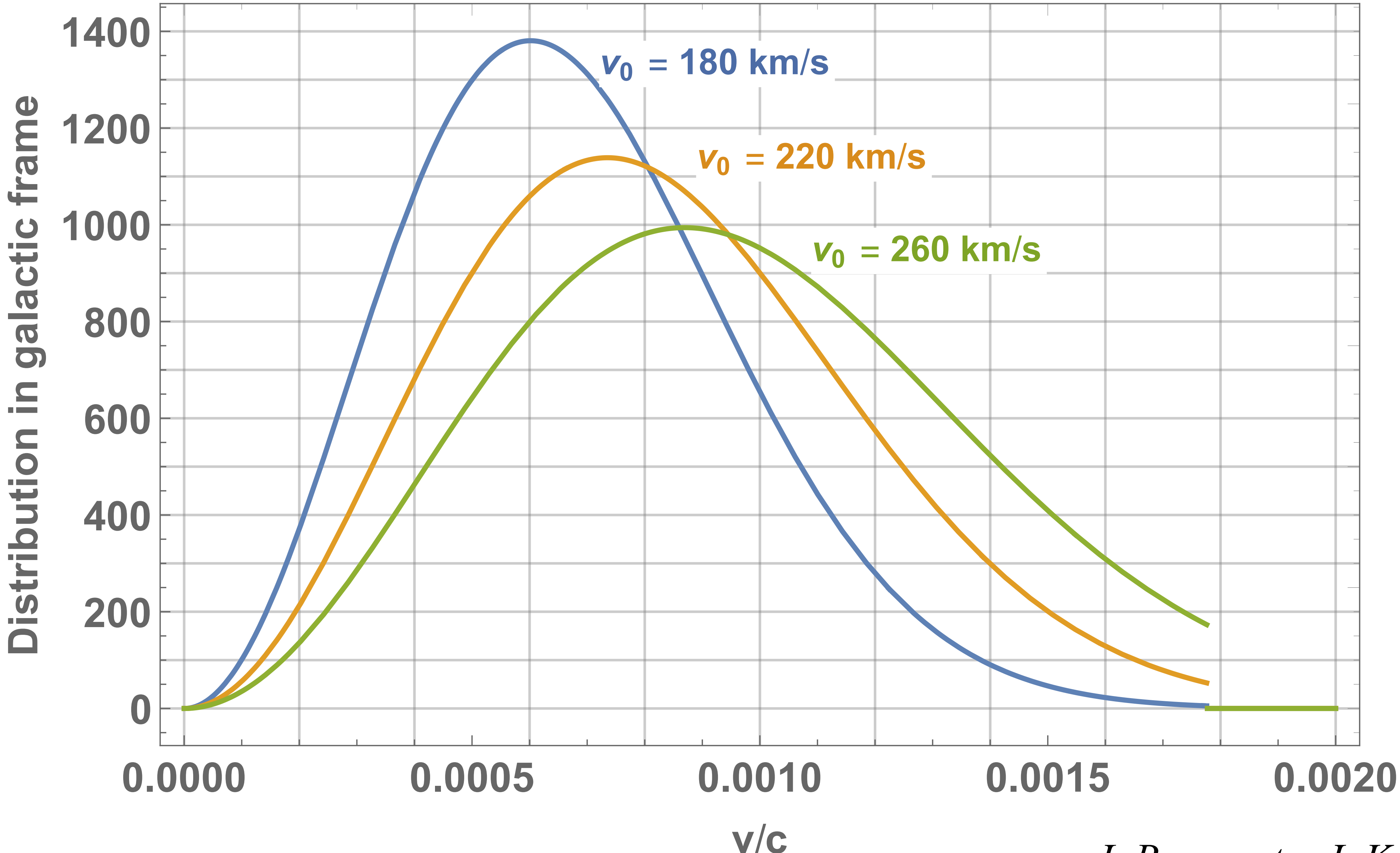

J. Bramante, J. Kumar, **N. Raj**
Phys Rev D **(2019)**

Pinpointing mean speed

galactic frame

$$f(v) = \frac{1}{\mathcal{N}} v^2 \exp\left(-\frac{v^2}{v_0^2}\right) \Theta(v_{\rm esc} - v)$$

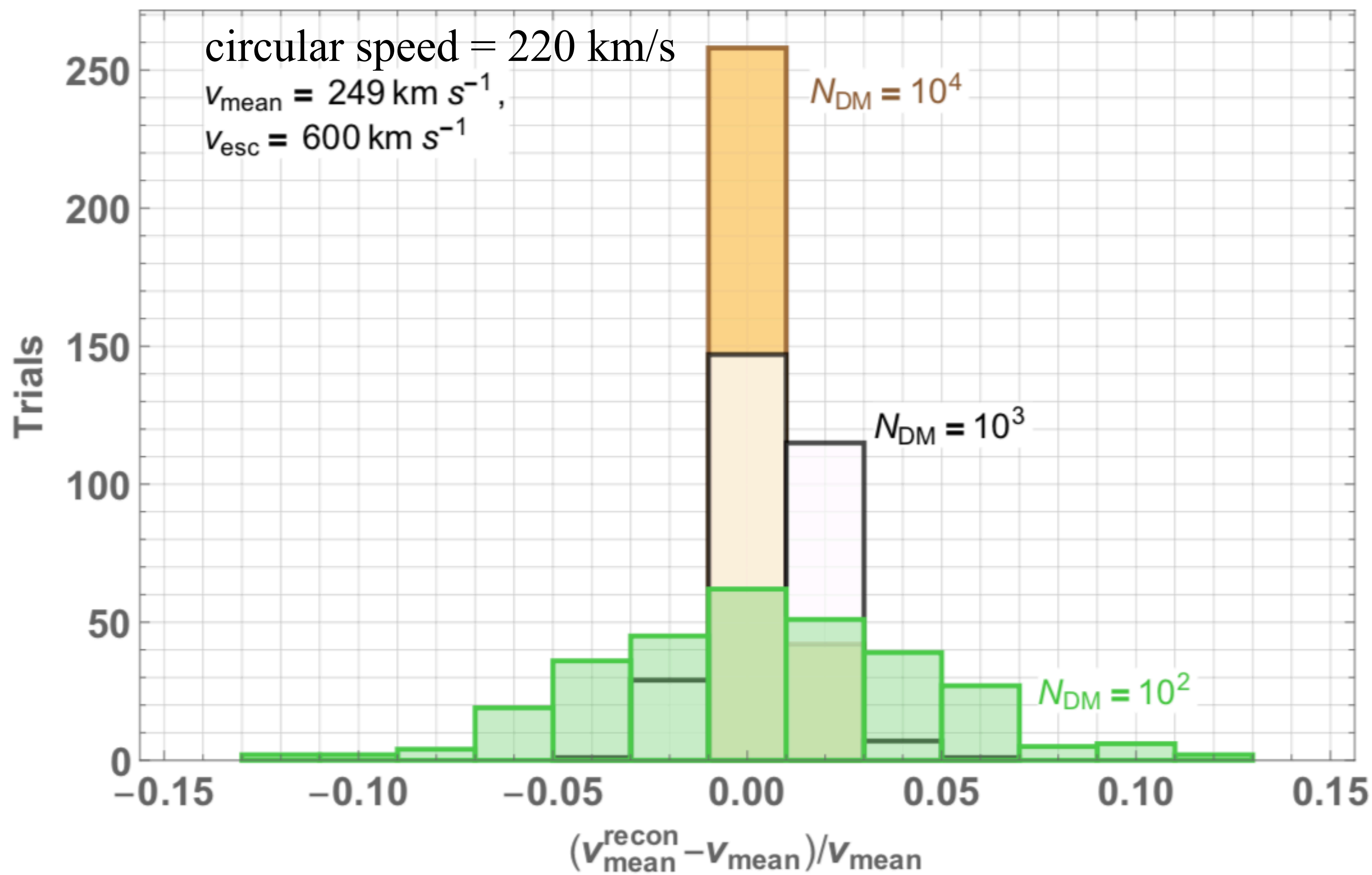

J. Bramante, J. Kumar, **N. Raj**
***Phys Rev D* (2019)**

Testing velocity anisotropies

galactic frame

angular distribution:

$$g(\theta, \phi) = c_{00} Y_{00} + c_{\ell m} \sum_{\ell=1,2} Y_{\ell m}$$

contribution

monopole ~ 1

dipole ~ ε

quadrupole ~ ε

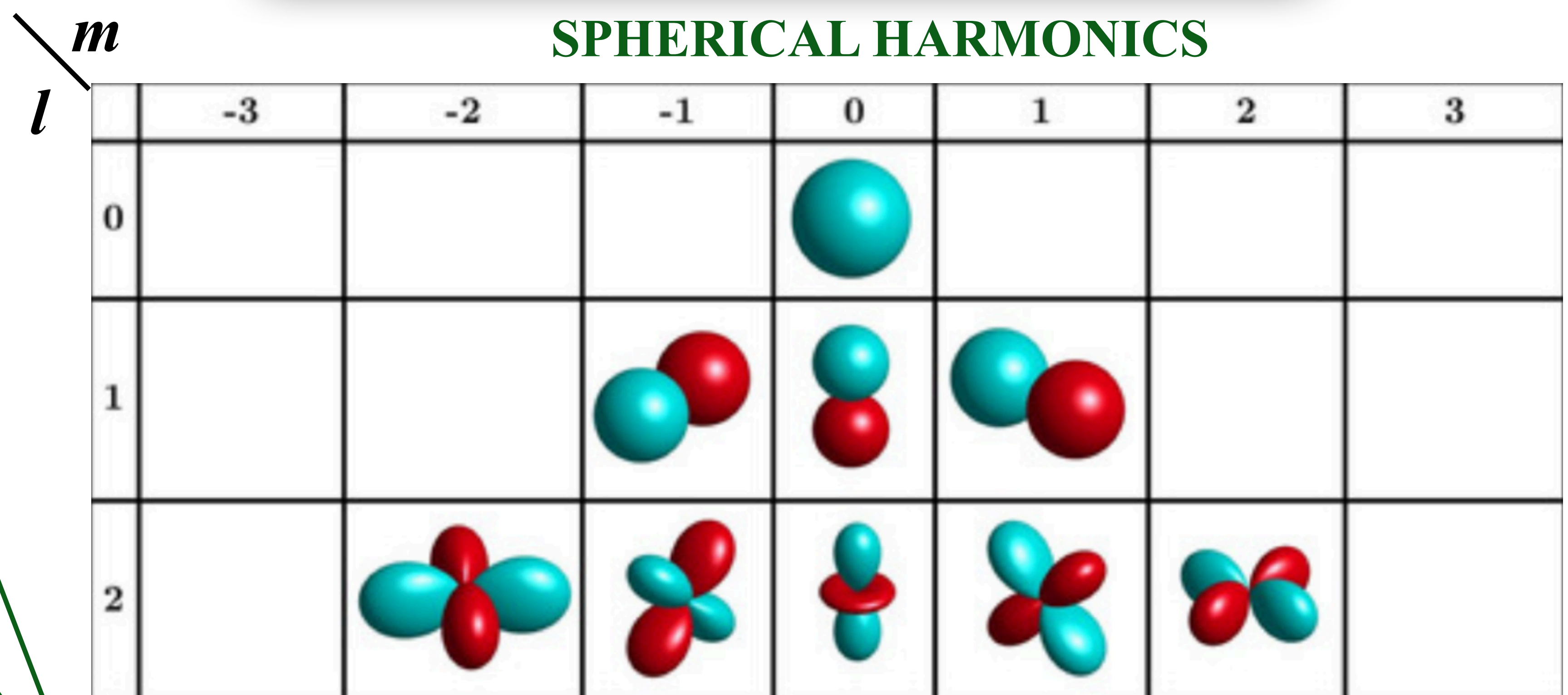

test anisotropy, ε << 1

Benchmark:

$$\varepsilon = 0.1 \quad => \quad c_{\ell m} = \begin{cases} \sqrt{1-\varepsilon^2}/\sqrt{1+7\varepsilon^2} = 0.962; \;\; \ell = 0, m = 0 \;, \\ \varepsilon/\sqrt{1+7\varepsilon^2} = 0.097; \;\; \ell \neq 0 \;. \end{cases}$$

J. Bramante, J. Kumar, **N. Raj**
***Phys Rev D* (2019)**

Testing velocity anisotropies

monopole coefficient | dipole coefficient

good angular resolution (smearing negligible)

poor angular resolution (smearing significant)

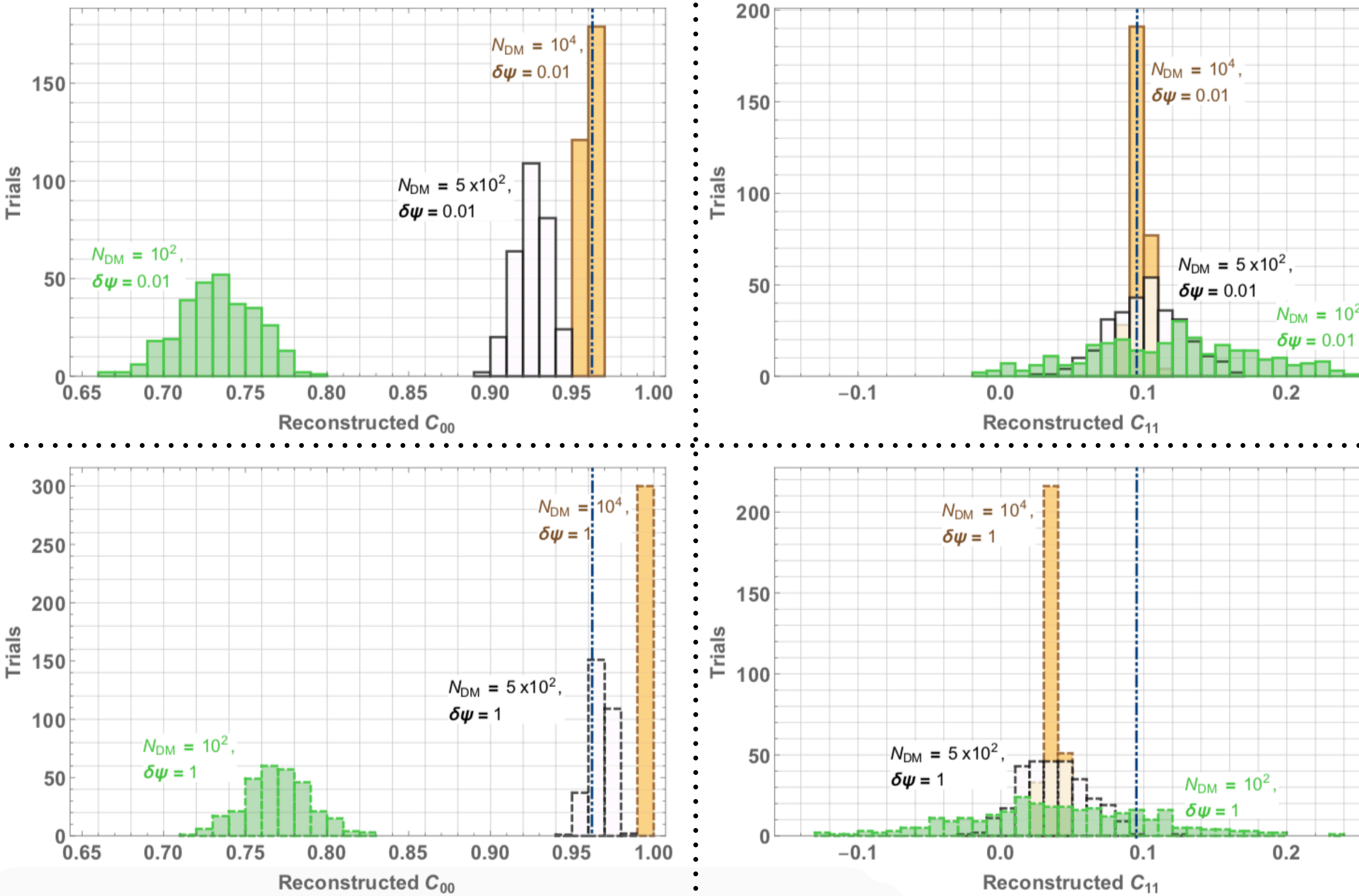

LESSONS: good statistics => accuracy & precision, smearing => anisotropies wash out.

J. Bramante, J. Kumar, **N. Raj**
***Phys Rev D* (2019)**